This is to certify that the

thesis entitled

THE EFFECT OF TRIPLE PELVIC OSTEOTOMY ON THE BIOMECHANICS AND ANATOMY OF THE HIP JOINT IN DYSPLASTIC DOGS
AN *IN VITRO* EXPERIMENTAL STUDY

presented by

Loic Marie Andre Dejardin

has been accepted towards fulfillment
of the requirements for

Master of Science degree in Small Animal Clinical Sciences

Major professor

Date 8-23-96

THE EFFECT OF TRIPLE PELVIC OSTEOTOMY ON THE BIOMECHANICS

AND ANATOMY OF THE HIP JOINT IN DYSPLASTIC DOGS

-

AN *IN VITRO* EXPERIMENTAL STUDY

By

Loic Marie André Déjardin

A THESIS

Submitted to
Michigan State University
in partial fulfillment of the requirements
for the degree of

MASTER OF SCIENCE

Department of Small Animal Clinical Sciences

1996

ABSTRACT

THE EFFECT OF TRIPLE PELVIC OSTEOTOMY ON THE BIOMECHANICS AND ANATOMY OF THE HIP JOINT IN DYSPLASTIC DOGS
-
AN *IN VITRO* EXPERIMENTAL SUDY

By

Loic Marie André Déjardin

The effect of triple pelvic osteotomy (TPO) on biomechanics, articular contact areas and joint coverage of dysplastic canine hips was investigated *in vitro* in an attempt to provide a scientific basis for selection of optimal acetabular ventroversion (AVV) angles. TPO was performed bilaterally (20°, 30° and 40°) in 9 dysplastic retrievers. Hip forces in the transverse plane were computed using a 2-dimensional static model. Joint contact and coverage were inferred from transverse scan images. Customized "hinge plates" were used to determine the minimal AVV angle providing hip reduction.

Hip forces significantly decreased from 0° to 20° of AVV while contact areas and coverage increased. Hip reduction consistently occurred before 20°. All variables remained virtually unchanged beyond 30° of AVV.

This study suggests that increasing AVV beyond 30° may not further improve TPO outcome and therefore should be carefully weighed against the increased risk of complications associated with large correction angles.

A Philippe et Solange

ACKNOWLEDGMENTS

First comes first: I wish to express my deepest gratitude to my Mentor: **Doctor Steven Arnoczky** for honoring me by presiding my Masters committee. Your confidence and enthusiastic support have been, during and beyond the completion of this project, a constant source of motivation and inspiration. I feel proud and privileged to benefit from your keen synthetic mind and strong scientific leadership and hope this work will reflect my appreciation.

I also would like to acknowledge the members of my committee: **Dr. Ruby Perry** for her professionalism, sagacious expertise, and... great sense of humor. I will always cherish my experience with you. **Dr. Charles DeCamp** for his supportive friendship and advice, both at professional and personal levels, since I started at Michigan State. **Dr. Bari Olivier** for his invaluable help with the statistical analysis, contagious enthusiasm and genuine interest in this work. **Dr. Robert Soutas-Little** for his patience and excellence in teaching me biomechanics and for his fine attention to details in reviewing this thesis.

I wish to thank **Dr. Peter Torzilli** for writing the computer software used in this study.

My thanks also go to **Mike McLean** (frame, hinge plates), **Dereck Fox** (drawings) and **Sharon Thon** (pictures) for their expertise and artistic talent.

Last but not least, merci a mon Pere **Philippe Dejardin** pour la fabrication du cadre prototype utilise tout au long de cette etude et pour m'enseigner l'amour du travail bien fait.

This work was supported by The **Laboratory for Comparative Orthopaedic Research** in the College of Veterinary Medicine at Michigan State University.

TABLE OF CONTENTS

LIST OF TABLES

LIST OF FIGURES

ABBREVIATIONS

AVV	Acetabular Ventroversion
CG	Center of Gravity
CHD	Canine Hip Dysplasia
CT	Computerized Tomography
DCP	Dynamic Compression Plate
FHO	Femoral Head Ostectomy
ITO	Inter-Trochanteric Osteotomy
OFA	Orthopaedic Foundation for Animals
THR	Total Hip Replacement
TPO	Triple Pelvic Osteotomy

INTRODUCTION

Canine hip dysplasia (CHD), an abnormal development of the hip joint, is a common orthopaedic disorder affecting mainly large, rapidly growing breeds of dogs[129]. While the precise etiology of hip dysplasia remains unknown, excessive hip laxity occurring as early as 2 weeks of age is considered the major factor responsible for the pathological changes characteristic of the disease[50, 124, 128]. Hip instability alters the distribution of the forces applied to the growing femoral head and acetabulum. The continuous alteration of the hip biomechanics affects bone remodeling and ultimately the conformation of the joint[2, 16]. As a consequence, hip subluxation develops, followed by severe secondary degenerative changes[72, 126]. Clinically, canine hip dysplasia is characterized by a painful crippling lameness, initially due to hip instability followed by progressive degeneration of the joint (osteoarthrosis) which occurs later in the course of the disease[130].

Canine hip dysplasia is considered a highly heritable, polygenic, multifactorial disease which severity depends on the proportion of affected genes as well as nutritional and environmental factors[16, 27, 28, 47, 50, 78, 143]. Indeed, factors such as overnutrition, high dietary calcium, vitamin D and/or vitamin C[11, 12, 46, 123, 129], excessive energy consumption[47, [78, 93, 123] or high dietary anion gap[62] have been shown to increase the frequency and the severity this disease.

Among the numerous factors implicated in the development of hip dysplasia, joint laxity has long been recognized as a key factor in the pathogenesis of the disease. Studies have shown that maintaining joint congruity until 6 months of age in genetically predisposed puppies was sufficient to prevent CHD[127, 128]. By 6 months, ossification has stiffened the acetabulum and the pelvic musculature (abductors and rotators), moreover, the supporting soft tissues (joint capsule and teres ligament) have gained enough strength to prevent hip subluxation[2, 129, 130]. Conversely, when joint instability is surgically induced in genetically normal immature dogs by tendonectomy of the obturator and gemelli muscles, hip dysplasia develops[127]. Nonetheless, both the specific cause of laxity as well as the minimal amount necessary to induce CHD continue to be the center of much debate and investigations[10, 52, 61, 62, 74, 77, 152, 153]. To this date, objective evaluation of passive hip laxity in normal versus dysplastic dogs of various breeds and ages, its translation in functional laxity and its value as a predictor of CHD remain controversial[36, 72, 152, 153].

Regardless of its cause, CHD is widely considered a mechanical disease due, in part, to the disparity between muscle mass and strength and overly rapid growth of the skeleton[125]. Although dogs are usually born with normal hip joints, the discrepancy between muscle and skeletal maturity as the animal grows results in a relative lack of muscle strength and loss of joint stability and congruity[2, 75, 124, 126]. In turn, joint instability alters the force concentration on the growing, malleable femoral head and acetabulum leading to anatomical changes such as coxa valga, increased anteversion and shallowness of the acetabulum[87, 134, 172]. Subsequently, as neither the femur nor the acetabulum are subjected to adequate loads, joint configuration and biomechanics are altered[8, 16, 49, 134]. As subluxation progresses over time, excessive loads are imposed to the articular cartilage and degenerative joint disease develops[72, 87, 119, 126].

Early signs of dysplasia include reluctance to exercise, lameness, gait alteration and muscle atrophy of the pelvic limbs. Because these signs are common to many orthopaedic conditions, final diagnosis of coxofemoral instability and CHD is usually proposed after specific examination tests and radiographic evaluation are performed. The Ortolani, Barlow and/or Bardens tests are commonly used to diagnosed CHD. The Ortolani test provides a quantitative estimate of coxofemoral laxity by measuring the abduction angles at which subluxation and reduction of the femoral head occur when axial pressure is applied to the femur[21, 101]. The Barlow test[8] is qualitative and essentially mimics the first phase of the Ortolani test (evaluation of hip subluxation). Finally the Bardens test[7] correlates lateral displacement of the femoral head to coxofemoral laxity. In addition, various imaging methods such as stress view radiographs[10, 152], dorsal acetabular rim radiographic view[149] and ultrasonography[42] have been developed to assess CHD. However, the gold standard by which CHD is evaluated remains the ventrodorsal, hip extended radiographic view as recommended by the Orthopaedic Foundation for Animals (OFA)[27,28]. Various radiographic parameters such as the Norberg angle (normal > 105°)[34], the Wiberg angle (normal > 15°)[82] or the percentage of femoral head coverage by the acetabulum (normal > 50%)[82] provide a quantitative evaluation of hip subluxation.

Alternatively, a distraction index reflecting passive laxity can be calculated from stress (distraction/compression) ventrodorsal radiographs (normal < 0.3)[152].

Treatment modalities essentially vary depending on the amount of osteoarthrosis present at time of diagnosis. Regardless, the therapeutic goals are to relieve pain and when feasible, improve or restore joint function in an attempt to limit the progression of osteoarthrosis[59, 121, 165, 172]. Both conservative and medical managements of hip dysplasia are usually indicated for young dogs early in the course of the disease or for older patients crippled by osteoarthrosis. Weight reduction, controlled exercise[59, 128] in combination with analgesics[69], anti-inflammatory[54, 103, 168] and/or chondroprotective agents[30, 76] constitute the core of the conservative approach to CHD. However, despite few reports of successful conservative management in young dogs[9, 151], it is generally accepted that, joint instability will eventually lead to irreversible degenerative articular changes and therefore should be surgically corrected as early as possible[139, 148, 172].

Various surgical protocols have been devised to treat hip dysplasia. Femoral head and neck ostectomy (FHO) was the first procedure recommended in the treatment of severely arthritic hips[96, 155]. Despite controversial modifications of the original technique[67, 69, 70, 116, 164], FHO remains a salvage procedure which main objective is the relief of pain, not the improvement of gait abnormalities[172]. Best results are observed in light-weight dogs when the procedure is performed unilaterally[13]. Recently, another salvage procedure has been described for the treatment of severe hip dysplasia. In this technique, a shelf arthroplasty using a biocompatible osteoconductive polymer is performed to extend the dorsal rim of the acetabulum and prevent hip subluxation[58, 142]. Recent studies have highlighted the numerous complications and unsubstantiated claims of this highly controversial procedure[71, 95, 167]. A better alternative in the treatment of severe hip dysplasia consists of replacing the mechanically deficient joint(s)[33, 79, 97, 104]. Total hip replacement, although technically more demanding than FHO, has become a widely performed and highly successful procedure[33, 79, 97, 99, 100, 104]. Immediate relief of pain and more importantly long term restoration of joint function has been achieved in more than 95% of the cases[98].

When hip dysplasia is diagnosed at an early stage, before secondary degenerative changes have occurred, pectineus myectomy and various corrective osteotomies can be performed. Myectomy of the pectineus muscle has been advocated to release the stress imposed on the joint capsule and increase the range of abduction of the hind limbs[51, 171, 172]. Increasing the range of abduction was thought to improve the articular contact between femoral head and acetabulum and consequently decrease the stress imposed on the articular cartilage. This procedure, however, does not improve joint stability and therefore does not prevent the progression of osteoarthrosis[172].

Conversely, osteotomy procedures such as intertrochanteric osteotomy (ITO) and triple pelvic osteotomy (TPO) were designed to transform the anatomical configuration of the immature coxofemoral joint in an attempt to alter the forces acting upon it. With postoperative improvement of joint stability and congruity, it is hoped that hips will develop normally under physiological loads. In turn, this may limit articular degenerative changes resulting from abnormal and/or excessive loading of the joint[87, 119].

Intertrochanteric osteotomy is recommended when hip dysplasia results from an abnormal development of the proximal femur[15, 17, 22, 170]. By modifying the femoral neck angle or the angle of anteversion, or both, ITO improves the mechanics of the abductor muscles[113]. Alternatively, a femoral neck lengthening procedure[32] and an acetabuloplasty technique[18] have been used to redirect and seat the femoral head deeper into the acetabulum. These latter two procedures, however, are considered hazardous or obsolete when compared to intertrochanteric osteotomy or triple pelvic osteotomy.

When insufficient acetabular coverage is seen as the primary deformity causing joint incongruity, triple pelvic osteotomy is recommended[53, 113, 139, 147]. In this technique, the acetabulum is reoriented so that the joint remains congruent throughout its functional range of motion[139, 140, 147, 148]. Specially designed plates are often used to stabilize the acetabulum at various angles of acetabular ventroversion (AVV). Currently, plates angled at 20°, 30° and 40° are available[148]. Although specific techniques may vary slightly, the rationale behind TPO is to improve joint congruity. However, it is thought that TPO could also help restore the normal biomechanics of the hip by decreasing the magnitude of the hip force and by increasing the contact area upon which this force is applied. This in turn should reduce the stress imposed on the articular cartilage to a level compatible with normal mechanical and cellular function and may help to prevent the development of coxarthrosis in immature dysplastic hips[136, 137, 157]. As a consequence, the later need for radical procedures such as FHO or THR could be lessened.

Over the past 15 years, TPO has gained popularity among veterinary surgeons as a valuable method to limit the progression of arthrosis in young dysplastic dogs. Clinical results have demonstrated subjective improvement in animals undergoing TPO[139, 147]. These results have been confirmed in experimental studies based on force plate analysis[83]. However, little is known about the effect of TPO on the hip biomechanics. Whether the procedure changes the magnitude and orientation of the forces acting about the dysplastic hip joint, modifies the articular contact area between acetabulum and femoral head, or both, have yet to be determined. Furthermore, despite known postoperative complications inherent to increased acetabular ventroversion[55, 64, 120, 140, 150, 161, 162], no guidelines have been recommended for practical selection of the optimal angle of acetabular ventroversion. Determination of the optimal angle of AVV necessary to maintain stable reduction of the hip could further the purpose of the TPO procedure by avoiding potentially harmful overcorrective approaches.

It is, therefore, the purpose of this thesis to investigate the effect of TPO on the biomechanics and configuration of dysplastic canine hips, in an attempt to provide a scientific basis for selection of the optimal angle of acetabular ventroversion in clinical situations. Three major hypotheses are evaluated in three distinct *in vitro* studies:

KINETIC STUDY

This study examines the effect of TPO on the magnitude and orientation of the forces acting about dysplastic hip joints. Our working hypotheses are as follow:

H1: Hip forces are increased in hip dysplasia

H2: TPO decreases the magnitude of the hip forces

These hypotheses will be tested using a previously described 2 dimensional mathematical model. Using a specifically designed computer software, the magnitude and orientation of the hip forces will be computed from pre- and postoperative radiographic measurements of canine pelvii and femora.

ANATOMICAL STUDY

This study analyzes the effect of TPO on articular contact areas between the femoral head and the acetabulum. The working hypotheses are:

H1: Articular contact area is decreased in dysplastic hips

H2: TPO increases articular contact between acetabulum & femoral head

To test these hypotheses, articular contact areas will be computed from anatomical measurements on pre- and postoperative transverse CT scan images of canine hip joints.

FUNCTIONAL STUDY

The functional study determines the minimal angle of acetabular ventroversion necessary to achieve stable reduction of hip subluxation. Our hypothesis is that:

H1: Reduction of hip subluxation occurs for AVV angles less than 20°

The minimal AVV angle at which stable hip reduction occurs will be determined using a custom designed "hinge plate" which allows for continuous increase of acetabular ventroversion.

LITERATURE SURVEY

HIP BIOMECHANICS

Functional anatomy

The functional anatomy of the hip joint has been thoroughly studied in both humans[87, 118, 119, 134] and dogs[6, 43, 44, 114, 133]. The following will briefly describe the anatomy of the hip, underscore significant differences between humans and dogs, and address the importance of joint forces in the development of the coxofemoral joint.

The hip is a "ball-and-socket" joint formed by the articulation of the femoral head with the acetabulum. Its configuration allows a wide range of motion mainly in flexion-extension but also in ab-adduction and internal-external rotation. The hip is powered by large muscle groups which help maintain balance in gait and permit locomotion. The femoral head forms two thirds of a sphere slightly flattened along the vertical direction, while the acetabulum resembles a cup deepened by the peripheral fibrocartilage labrum. As a result, the hip is intrinsically stable, although slightly incongruous, under no or light loads. The horseshoe shape of the acetabulum allows this structure to deform (spread) under load. This, in addition to the flattening of the femoral head, improves the congruity of the joint, increases its load bearing surface, and insures minimal stress on the articular cartilage[86]. Conversely, lack of adequate bony configuration, such as slanting of the acetabular roof, leads to dislocation of the joint and degenerative joint disease.

Femoral neck angle and angle of anteversion describe the relative position of the femoral head with respect to the diaphysis of the femur. These angles, respectively, approximate 125° and 12° in humans, and 135° and 13° in dogs. However, large variations, in part due to the method of measurement[43, 44, 133], have been reported. The configuration of the hip in adult humans has been described by Radin[119]. The femoral neck angle and, to a lesser extent, the lateral flair of the iliac wings, determine the length of the lever arm of the abductor muscles. Coxa vara increases this length, thus giving the abductor muscles a mechanical advantage as they counterbalance body weight during one-leg stance. Consequently, both the abductor muscle force and hip reaction force are diminished. Extreme varization (reduction of the femoral neck angle), however, limits abduction. Conversely, coxa valga affects hip adduction and reduces the abductors lever arm, thus decreasing their mechanical efficiency. Consequently, the magnitude of the hip reaction force also increases. Unlike humans, dogs do not need strong abductor muscles to maintain pelvic equilibrium. The abductors lever arm is therefore relatively shorter than in humans as demonstrated by a smaller trochanter and the craniocaudal orientation of the iliac wings. In the sagittal plane, the angle of anteversion provides the gluteus maximus with a lever arm which amplifies its effectiveness. Excessive anteversion, however, promotes cranial luxation of the hip and limits external rotation of the femur.

Development of the hip joint

The eventual shape of the hip joint is determined by the distribution of gravitational and muscle forces and represents a compromise between its load carrying function and locomotion needs[87, 127]. Morris[87] and Rydell[134] reported that, in humans, the femoral neck angle changes from 150° in newborns to 125° in adults, while the angle of anteversion gradually decreases from approximately 23° to 12°. Both authors attributed the larger femoral neck angle and anteversion angle in newborns to uterine pressure and absence of gravitational forces during gestation. As a result of weight-bearing, both valgus and anteversion decrease gradually to adult values. While anteversion results from forces exerted in the transverse plane (rotators), the magnitude of the femoral neck angle is dictated by forces (gravity, abductors) applied to the femoral head in the frontal plane. Valgus deformity, usually associated with increased femoral anteversion, proceeds from inadequate loading of the immature hip and results in joint instability[87, 134]. Coxa valga is often observed in congenital dislocation of the hip. Conversely, coxa vara, usually associated with decreased anteversion, has minor pathological effects[87].

Using a 2-dimensional biomechanical model of the growing human hip, Heimkes described the forces acting on the capital epiphysis and greater trochanter apophysis during one-legged stance[49]. In Heimkes' model, the force developed by the vastus lateralis is considered in addition to body weight and abductor force already described by Pauwels[105]. The proximal femur is, therefore, subjected to the hip reaction force (vectorial sum of body weight and abductor muscle force) and to the trochanteric resultant force (vectorial sum of lesser glutei and vastus lateralis muscle forces). Consequently, the greater trochanter is exposed to a compressive force (about 1.7 times body weight) exerted by the combined action of the hip abductors (lesser glutei) and part of the knee extensors (vastus lateralis). As Pauwels[110] showed the orientation of the capital physis to be perpendicular to the hip reaction force, Heimkes resolved that the trochanteric resultant force is perpendicular to the physis of the greater trochanter (Figure S1)[49]. Heimkes observed that changes in the orientation of the trochanteric resultant force, regardless of the cause (paralysis, lack of weight-bearing), alter the orientation of the trochanteric physis and inhibit the craniolateral growth of the trochanter[49]. This, in turn, decreases the lever arm, thus mechanical effectiveness, of the abductor muscles and alters the direction of the abductor force towards the vertical. Consequently, the magnitude and verticality of Pauwels' hip reaction force also increase and coxa valga develops. From these observations, Heimkes concluded that the greater trochanter is of utmost importance in the development of the hip joint[49].

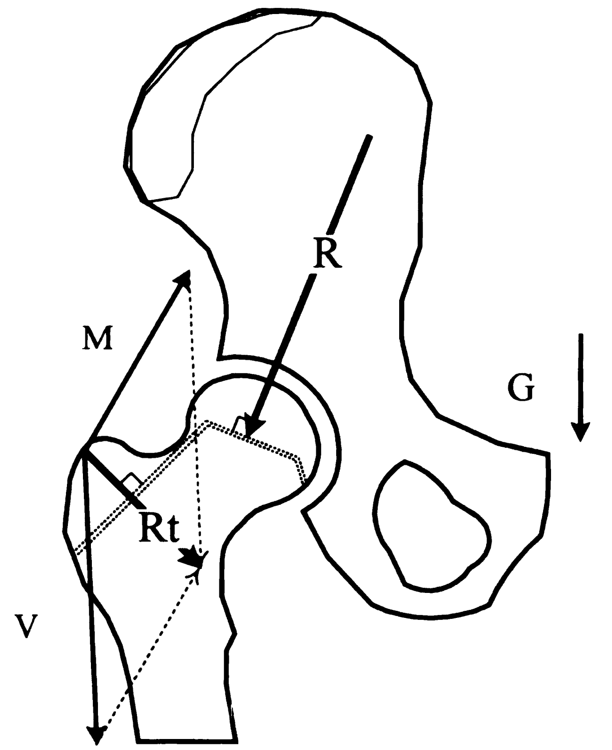

Figure S1 - Vector diagram of the forces acting upon the proximal femur according to Heimkes[49]. The trochanteric resultant (Rt) is the vectorial sum of abductor muscle force (M) and vastus lateralis muscle force (V). Similarly, the hip reaction force (R) is the vectorial sum of abductor muscle force (M) and gravitational force (G)[109]. Both resultants (Rt and R) act perpendicularly to their respective physes (i.e. trochanteric[49] and capital[110]).

Biomechanics of the normal hip

Pauwels[105, 108, 109] is credited with being the first scientist to propose a theoretical model that describes the biomechanics of the human hip. In Pauwels' model, the magnitude and orientation of the forces acting about the hip in the frontal plane are inferred from the analysis of anteroposterior radiographs. Anatomical measurements of the inclination of the abductor insertions, positions of the center of gravity (CG) of the body, and the center of rotation of the femoral head, translate in angles and lever arms, thereby allowing calculation of the forces acting on the hip.

In humans, maintaining pelvic balance requires that external gravitational forces be counteracted by internal muscle forces developed by the hip abductors. Therefore, during the one-legged stance, the femoral head acts as the fulcrum of a lever system. Using force diagrams and assuming that the CG of the body lies in the frontal plane passing through the hip, Pauwels demonstrated that, in one-legged stance, body weight (G) acting through a lever arm (a) and abductor muscle force (M) acting through a lever arm (b) are in equilibrium. Thus, G x a = M x b (Figure S2). Also, Pauwels resolved that the hip reaction force is the vectorial sum of body weight and abductor muscle force. Therefore, the load imposed on the hip, is higher than body weight[105]. The hip has been compared to a nut in a nutcracker since it is caught between the downward pressure of the body weight and the upward pull of the abductor muscles[31]. Indeed, pelvic equilibrium requires contraction of the abductors which increases the load on the hip joint to 2.5 [31, 57] to 3 times body weight[105]. These values have been confirmed *in vivo* by Rydell[135].

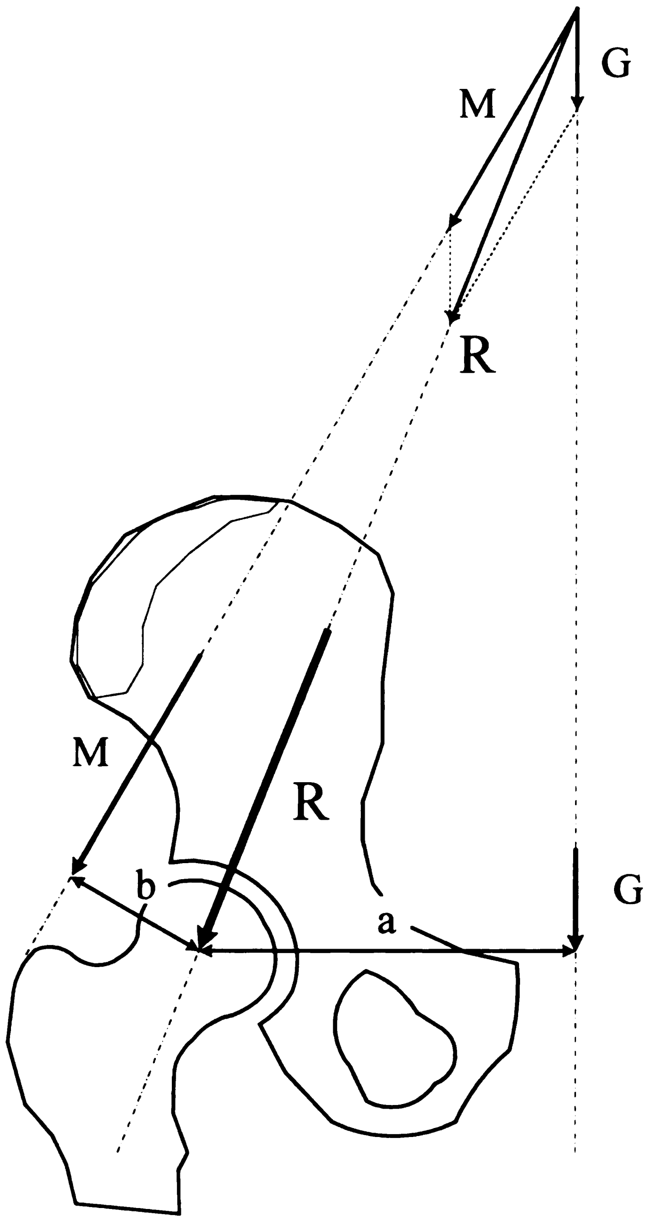

Figure S2 - Vector diagram of the static forces acting upon the hip joint according to Pauwels[109]. Partial body weight G* acts about the hip through its lever arm a while the abductor muscle force acts through the lever arm b. In a state of equilibrium, Gxa = Mxb. The hip reaction force R is the vectorial sum of the abductor muscle force (M) and the partial body weight (G).

---

*G corresponds to body weight minus the weight of the supporting leg.

In addition, Pauwels determined that in normal hips, the orientation of the hip reaction force (165° from the vertical), parallels that of the medial trabecular system of the femoral neck[109]. From these observations, Pauwels inferred that the femoral neck is subjected to compressive and bending stresses and later confirms this "bending theory" using photoelastic models[110]. The effect of coverage of the femoral head by the acetabulum on stress distribution and magnitude was also studied by Pauwels[106]. The study concluded that decrease in hip coverage increases the magnitude of compressive articular stresses especially at the level of the dorsolateral acetabular labrum.

In an effort to further determine the static forces on the human hip, Inman[57] calculated the value of the theoretical torque (moment) exerted by the abductor muscles then checked this value experimentally using electromyography. The theoretical torque was consistently one half greater than the experimental torque. Only with the pelvis elevated 15° on the non weight-bearing side did the theoretical and experimental torques agree. Inman concluded that the force preventing the pelvis from rotating about the supporting hip is not entirely due to muscle pull. The discrepancy between the theoretical and experimental torques was attributed to the passive tension of the fascia lata and iliotibial band due to the pelvis sagging during the experiment. According to Inman, elevation of the pelvis cancels the tension of the fascia lata so that pelvic equilibrium is solely maintained by the abductors which then develop a force of approximately 1.5 times body weight. Inman further resolved from electromyographic activity (or lack thereof), that with the pelvis sagging 15°, the moment induced by body weight was almost entirely resisted by tension of the fascia lata and iliotibial band. Kummer[65] later resolved that the abductorial force was composed by the forces of the lesser glutei (70%) and the iliotibial band (30%). More importantly, Inman determined that regardless of the relative contribution of the abductor muscles and ligaments, the hip reaction force was constant and independent of pelvic inclination. The theoretical and experimentally calculated hip reaction force was 2.5 times body weight. Furthermore, the orientation of the hip force (165° from the vertical) coincided with the medial trabeculae of the femoral neck, thus validating Pauwel's analysis of hip biomechanics.

The bending theory of the femur has been challenged by various investigators who reasoned that the femoral neck is actually loaded in compression[57, 90]. Observing that abductor and tensor fascia lata muscles exert a force oriented along the lateral trabeculae, Inman[57] resolved that both trabecular networks reflect the functional adaptation of the femoral neck to compressive stresses (Wolff's law). This refutes the original "crane" analogy formulated by Meyer[84] and endorsed by Pauwels, according to which the medial system resulted from compressive forces while the lateral system was subjected to tensile loads. According to Inman, the orthogonal orientation of the lateral and medial trabeculae distally, suggest that bending only occurs in the subtrochanteric area.

Assuming that functional adaptation of bones should lead to a bending-free skeletal scaffold, Moser[90] introduced a system of tear strings to demonstrate that the femoral neck is loaded in compression. In this model, muscles are recruiting tear strings which can resist tensile stresses so that segments of the skeleton are solely loaded in compression along their longitudinal axes.

In a critical analysis of Pauwels' bending theory, Kummer[65] used computer-aided graphical static analysis, photoelastic technology and radiodensitometry to evaluate both architecture and stress pattern of the proximal femur. This study confirmed Pauwels' results by demonstrating that hip forces are the smallest in coxa vara and increase in coxa valga. Conversely, the stress pattern in the femoral neck is lower and more uniform in coxa valga and higher, especially in tension, with coxa vara. Similarly, the stress diagram of the acetabular roof varies with femoral neck angles. While uniform in hips with normal femoral neck angle, stress concentration slightly decreases laterally in coxa vara and greatly increases laterally in coxa valga. From these results, Kummer observed that, regarding abductor force and acetabular stress, coxa vara is optimal but, with respect to stress in the femoral neck, coxa valga is more beneficial[65]. Kummer inferred that bending of the femoral neck could be annulled only by steady recruitment of the abductors. However, constant contraction of the abductors would not only increase the magnitude of the hip reaction force considerably but would also shift its position over the acetabular rim, thus causing a large increase in articular stress. Considering optimization of muscular activity and articular stressing, Kummer concluded that a bending-free scaffold (as proposed by Moser) although theoretically possible, would lead to unfavorable stress distribution in the hip joint and may not be applied to human skeleton as a whole[65].

In an investigation of the mechanics of normal and arthritic hips, Bombelli[14] challenged Pauwels' theories. The author first hypothesized that mechanical equilibrium about the hip requires that the acetabular weight-bearing surface (i.e. acetabular sourcil) be horizontal. Then, based on the observation of bone density and orientation of the trabecular projections of the acetabular sourcil, Bombelli suggested that the dominant forces acting about the hip are always perpendicular to the weight-bearing surface of the acetabulum. Therefore, these forces should be vertically rather than obliquely oriented. Accordingly, Bombelli decomposed Pauwels' hip force in its vertical and horizontal component, however he split the reaction force with respect to the plane of the acetabular sourcil. Thus, only when the sourcil is horizontal, will the component vectors oppose each other. Since magnitude and orientation of the hip force do not depend upon size or shape of the acetabular weight-bearing surface[57], Bombelli concluded that, with inclination of the acetabular sourcil, the "expulsive" (horizontal) component of the hip force becomes unopposed and luxation occurs. In this theory, Bombelli used two reference systems to analyze the hip force and its reaction, and did not consider the equally unopposed vertical component of the hip force.

In order to analyze the biomechanics of the canine hip, Arnoczky and Torzilli[3] developed a theoretical model extrapolated from Pauwels' theory. In this model, the specifics of the quadrupedal stance were considered. Indeed, as quadrupeds, dogs have the ability to develop a spinal torque which acts in conjunction with the abductor muscles to balance the pelvis during 3-legged stance. The study concluded that the weight-bearing hip in a 3-legged stance is subjected to a force of almost 1.5 times body weight. Arnoczky further determined that the hip force increases with coxa valga, abduction, and subluxation of the hip, whereas it decreases with varization of the femoral neck and with hip adduction. Finally, Arnoczky demonstrated that the inclination of the hip forces increased towards the vertical with coxa valga and joint congruity. Its orientation in a normal hip was 69° from the horizontal, which, as in humans, closely coincides with the orientation of the medial trabecular system of the femoral neck. Joint contact areas were not investigated is this study.

The clinical importance of joint pressure has been underscored by Prieur[114] who reported that the load on the supporting hip varies from 3 times body weight during walking to more than 6 times body weight during jumping. Since the loaded hip joint area is approximately 1.5 cm^2 for a 30 kg dog, Prieur inferred that, in normal dogs, articular stresses can reach 120 kg/cm^2 (11.76 MPa) during physiologic activity and suggested that joint stresses may increase in hip dysplasia due to a decrease in articular contact area and an increase in the magnitude of the hip forces. Prieur also emphasized the correlation between changes in stress distribution on the acetabulum and changes in the orientation of the hip force due to hip dysplasia[114].

Biomechanics of the diseased hip and its treatments

In congenital dislocation of the hip, Radin[118] and Moseley[89] reported that hip subluxation results in the loss of the fixed fulcrum of the abductors. Furthermore, their lever arm (with respect to the geometrical center of the femoral head) is decreased while that of body weight is increased. This deprives the abductors of mechanical efficiency, alters the direction of their pull, and limits the range of motion of the joint. Subluxation also shortens the abductors, thus further diminishing their power. Since the development of the hip depends on the direction and magnitude of the forces applied to it[49, 87, 134], alteration of the joint anatomy and configuration occurs (shallowness of acetabulum, loss of head sphericity, coxa valga and increased neck anteversion). Coxa valga results from the lack of upward pull on the trochanter by the abductors and from the loss of compressive forces on the femoral neck. Anteversion increases due to the relative mechanical advantage of the hip extensors over the flexors in subluxation.

Abnormal joint loading increases the mechanical stress on the articular cartilage and over time leads to osteoarthrosis[87, 119]. Compressive stresses on the hip can be reduced by decreasing the load on the joint via simple means such as weight loss, use of a cane or the conversion to an antalgic gait[87, 107, 118]. For example, elevating the pelvis or leaning the trunk over the weight-bearing hip may annul the moment generated by the gravitational force so that little or no abductor muscle force is necessary to maintain pelvic balance. This results in a characteristic gait known as Trendelenburg gait[87]. Conversely, dropping the pelvis or leaning away from the supporting hip increases the moment arm of the body weight. This increases the magnitude of the abductor muscle force needed to sustain pelvic equilibrium and, in turn, increases the hip reaction force. Cartilage stress can also be surgically reduced by decreasing the abductor force via an increase of its lever arm (femoral osteotomies) or by increasing the weight-bearing area of the joint (pelvic osteotomies)[107]. The rationale of the various treatments of congenital hip dislocation in children have been thoroughly described[89, 108, 117, 118].

Biomechanics of closed reduction

Closed reduction is performed in infants and aims at restoring normal hip stresses during growth[118]. Postoperative abduction helps to stabilize the hip, redirects and reduces abductor force, and minimizes the subluxating component of the hip force. While abduction does not increase the containment of the femoral head, it does provide a better coverage of its weight-bearing surface. Performed prior to 18 months of age, closed reduction and controlled abduction have the potential to normalize hip development[138].

Biomechanics of varus osteotomies

Both varization of the femoral neck and lateralization of the trochanter improve the mechanical effectiveness of the abductor muscles by increasing the torque they create[118]. Similarly, body weight works through a lever arm extending from the CG to the center of the femoral head. The work of the abductor in maintaining pelvic equilibrium can be reduced by shortening the lever arm of the body weight (Trendelenburg gait) or by increasing that of the abductors (varus osteotomy)[105, 108]. Varus osteotomy also redirects the abductor muscle force (decreasing its vertical orientation), thus reducing the vertical component of the hip reaction force which tends to luxate the hip from a shallow acetabulum. Although containment of the femoral head is unchanged by the procedure, the hip force is reoriented so that it is distributed over a larger contact area. The beneficial effect of varus osteotomy has been criticized by Moseley[89] who observed that the mechanical benefit of increasing the lever arm of the abductors is at least partly offset by the reduction of the functional length of the muscles. However, according to Moseley, a minor indirect advantage of the procedure is the slight increase in femoral head coverage secondary to the pelvic tilt that results from the shortening of the operated leg. Varus osteotomies have been advocated by Pauwels[107] and Maquet[80] in order to increase the lever arm of the abductors and reduce their tension.

Biomechanics of pelvic osteotomies

The principle behind pelvic osteotomies is to redirect all, or a portion, of the acetabulum so that tendency for hip subluxation is reduced in weight bearing positions[136]. Although these procedures may change the magnitude and orientation of the hip reaction force through medialization of the femoral head, their major effect is to increase the acetabular coverage of the femoral head so that the hip force is distributed over a larger acetabular area[118, 136]. Furthermore, improvement of femoral head containment ensures stable reduction of the hip joint, thus providing a fixed fulcrum around which the hip muscles can act effectively[118]. Although innominate osteotomies are not designed to improve abductors efficiency, severe medialization of the acetabulum such as in Chiari's procedure[25] increases the lever arm of these muscles. However, as in varus osteotomies, the mechanical advantage thus provided may be offset by the decrease in the functional length of the abductors. While single innominate osteotomies rotate the acetabulum laterally and anteriorly, other procedures such as periarticular osteomies[37] or Chiari's osteotomy shift the hip medially thereby increasing the lateral coverage of the femoral head and decreasing the lever arm of the gravitational force. Indeed, an investigation of the biomechanical effects of Salter's procedure by Rab[117] concluded that rotation of the innominate bone may reduce the lever arm of the body weight by up to 16%. This, in turn, increases the capacity of the abductors to support the pelvis and decreases the magnitude of the hip force. With TPO, the beneficial mechanical effect of medialization of the acetabular fragment was underscored by Ganz[37] who proposed a new periarticular osteotomy for the treatment of hip dysplasia.

Moseley[89] associated hip coverage with the center-edge angle, (formed by the horizontal and the line joining the acetabular rim and the femoral head center), and emphasized the fact that a hip can be well covered and stable, but poorly congruent and therefore subjected to high and heterogeneous compressive stresses. Thus, the closer the line of action of the hip force to the acetabular lip, the higher the risk of subluxation and the higher the articular cartilage stress. This confirms Pauwels' observations[106] of photo-elastic hip models which showed that increasing the center-edge angle from 0° to 90° decreases compressive stresses from 225 kg/cm^2 (22.05 MPa) to 18 kg/cm^2 (1.76 MPa).

PELVIC OSTEOTOMY PROCEDURES

Pelvic osteotomies in humans

Conservative treatment of congenital dislocation of the hip within the first year of life has been shown to be effective in restoring normal joint growth[26, 89]. With age however, as growth potential decreases, normalization of the hip biomechanics through acetabular remodeling does not occur[26]. Therefore, later in life, corrective procedures (pelvic osteotomies) aimed at reconstruction of the acetabulum become indicated [23].

Many pelvic osteotomies have been designed for the treatment of acetabular dysplasia in humans. These include single[60, 85, 136], double[163] and triple[157, 166] innominate osteotomies as well as periarticular osteotomies[37, 111, 169]. Improvement of joint congruence following early pelvic osteotomy normalizes hip stresses and allows the acetabulum to remodel. Restoration of the normal hip configuration also exerts a beneficial effect on the development of the upper femur[49, 141]. Indeed, with proper reorientation of the acetabulum, femoral anteversion and neck angles may decrease up to 20° and 10° respectively. Pelvic osteotomy procedures, however, are only recommended for the treatment of acetabular dysplasia and should be combined with femoral osteotomies if anteversion exceeds 70°, if femoral neck angle exceeds 160°, or both[141].

In single procedures, a transiliac osteotomy is performed dorsal to the acetabular roof, while the pubis and ischium remain intact. Then, the acetabulum is tilted laterally by inserting a trapezoidal bone graft[85, 136] or by performing a wedge osteotomy[60]. The latter procedure prevents lengthening of the limb as seen with Salter's innominate osteotomy. Following single osteotomies, expected improvement in lateral coverage is at best 15 degrees[60]. Therefore, these procedures are mainly indicated in young children (less than 3 years of age) with mild hip dysplasia, (i.e. when the slope of the acetabular roof does not exceed 35°). Regardless of the technique, single procedures are implemented before exhaustion of the remodeling capacity of the acetabulum through the triradiate cartilage[23].

As dysplasia worsens, the slope of the acetabular roof increases and permanent hip luxation occurs. In severe cases of congenital hip dislocation, double[163] and triple[157, 166] osteotomies involving the pubis and ischium are recommended to achieve greater angular correction. With periarticular pelvic osteotomies the largest acetabular corrections can be obtained while retaining pelvic canal integrity[37, 169]. Moreover, lateromedial displacement of the acetabulum can be controlled by varying the pivotal axis of the acetabular fragment from distal to proximal[37] or by performing a wedge osteotomy of the ilium[169]. Medialization of the acetabulum further improves the biomechanics of the hip by reducing the lever arm of body weight[37]. In addition, various periarticular spherical osteotomies extending into the triradiate cartilage have been devised to increase coverage of the femoral head without altering pelvic geometry[111, 169]. However, due to their technical complexity and risk of physeal damage, these procedures are seldom used.

In severe cases of hip dysplasia, extreme medialization of the acetabulum may be necessary to achieve adequate containment of the femoral head[24]. In Chiari's procedure, pelvic osteotomy is performed through the dorsal acetabular roof and the distal fragment containing the hip is shifted medially. Thus, the cut surface of the proximal segment lies directly above the medially displaced femoral head. This provides an extra-articular, dorsolateral shelf which prevents dorsal hip subluxation and improves joint containment, even in presence of severe osteoarthrosis[118, 156]. A major concern with this operation, especially in younger women, is the resultant severe narrowing of the pelvic canal.

A synopsis of the major innominate osteotomy procedures used in human and veterinary medicine is provided at the end of this chapter (Figure S3). Indications with respect to age of the patient, severity of the lesions, or amplitude of the acetabular ventroversion are also reported.

Prognosis following surgical treatment of congenital hip dislocation is usually guarded as surgical corrections only delay the onset of osteoarthrosis[137]. This underscores the importance of conservative treatment before 18 months of age. In fact, best results are expected if surgery is performed during infancy when rapid growth allows optimal remodeling of the acetabulum[111, 136]. Indeed, Salter[138] reported good long term results with single innominate osteotomy and emphasized the importance of age at time of surgery. However, even invasive procedures (i.e. shelf arthroplasties or triple pelvic osteotomies) performed on adolescents have been shown to delay the progression of coxarthrosis for approximately two decades[25, 157].

Recurrence of dislocation resulting from failure to achieve concentric reduction is the most common postoperative complication[162, 169]. Avascular necrosis and triradiate physeal arrest are infrequent complications but can severely jeopardize the outcome of periarticular procedures[37]. Other reported complications include sciatic nerve injury, reduction of the pelvic inlet (Chiari's procedure), implant failure, and infection[156].

Pelvic osteotomies in dogs

In an effort to relieve pain and restore limb function in dysplastic dogs, many pelvic osteotomy procedures have been developed in veterinary medicine[29, 53, 139, 147]. As in humans, pelvic osteotomies are designed to improve joint stability by rotating the acetabulum laterally, thus providing greater dorsal coverage of the femoral head[53]. These procedures are indicated in immature animals that present with a painful lameness related to hip subluxation. Best results are achieved when surgery is performed prior to 9 months of age and in the absence of degenerative joint disease[18, 53, 94]. These procedures presuppose that the femoral anatomy is normal (i.e. normal neck and anteversion angles).

Hohn's procedure[53] combines a step-like osteotomy of the ilium and an osteotomy of the ischial table. The ilium is then displaced laterally and stabilized with a lag screw. Since the acetabulum remains attached to the pelvis, this double pelvic osteotomy offers a limited degree of acetabular rotation and results in lateralization of the acetabulum. According to Hohn, hips treated with this technique do develop osteoarthrosis but to a lesser extent than the uncorrected joints[53]. A variation of Hohn's procedure was suggested by Stoll[159]. In this technique, the pubic symphysis rather than the ischium is cut in an effort to improve the degree of acetabular rotation.

Brinker's acetabuloplasty[18] is a procedure similar to the periarticular osteotomies devised in humans. In this technique, an incomplete circular osteotomy is performed parallel to and approximately 5 mm medial to the acetabular rim. The acetabulum, which remains attached to the pelvis medioventrally, is then tilted laterally by wedging a bone graft into the osteotomy site. While the design of the technique inherently limits the degree of acetabular rotation, good results have been reported in young dogs with mild hip dysplasia[18].

Triple pelvic osteotomy was introduced in veterinary medicine by Datt and Rudy in 1966[29]. In this technique, larger acetabular corrections can be achieved through a transverse osteotomy of the ilium performed along with pubic and ischial osteotomies. Thus freed, the acetabulum is rotated laterally approximately 20° to 25° and stabilized to the ilium with a bone plate. Excellent results have been reported by Datt and Rudy even when the procedure was performed in mature animals[29].

A combination of the pelvic osteotomies of Hohn and Rudy was described by Schrader[139, 140]. Through a single, dorsal-open approach to the hip joint, this technique combines step osteotomy of the ilium with pubic osteotomy and ischial osteotomy to achieve lateral rotations of the acetabulum as large as 70° to 90°. Schrader observed that, in order to achieve hip stability, 60° to 70° of acetabular rotation was usually required. Excision of the teres ligament, capsulorrhaphy and distal relocation of the trochanter complete the procedure. Using subjective evaluation, Schrader reported satisfactory results in 93% of the operated hips. However, gait alterations, restricted range of motion (especially in abduction) and crepitus were present in most instances. Schrader attributed the poor results to a loss of hip mobility (especially in dogs with large anteversion angles) and to muscle tension when reimplantation of the trochanter was performed too distally.

In an *in vitro* study comparing Stoll's and Schrader's techniques, Pijanowsky[112] demonstrated that Stoll's procedure results in greater acetabular rotation. The author concluded that, at least theoretically, this procedure provides better joint stability.

In 1986, Slocum[147] proposed a modification of Schrader's procedure. In this technique, a transverse rather than step osteotomy is performed perpendicular to the long axis of the ilium. The acetabular branch of the pubis is fully resected and the ischial table is osteotomized lateral to the obturator foramen. The procedure is performed through 3 separated approaches and often includes a pectineal myectomy. In the original technique a dynamic compression plate (DCP) was used to stabilize the ilium. The plate was twisted to a predetermined angle of axial rotation inferred from preoperative values of the Ortolani test. Satisfactory acetabular rotation is achieved when no subluxation is obtained beyond 10° of abduction with the femur axially loaded[147]. Since the description of the original technique, Slocum has suggested various improvements in order to facilitate acetabular rotation and limit alteration of pelvic geometry[148, 150]. The iliac osteotomy is now performed perpendicular to the long axis of the pelvis rather than ilium and special plates pre-angled at 20°, 30° and 40° (initially 45°) rather than twisted DCPs are used to stabilize the pelvis. The substitution of the 45° plate by a 40° plate reflects the current trends in surgical recommendations. Indeed, subsequent reports by Slocum[148, 150] emphasized the importance of avoiding overrotation of the acetabulum as a means to reduce postoperative complications. Such complications include neck impingement in abduction with subsequent ventromedial luxation of the femoral head and limited range of motion especially in abduction. Consequently, in contrast to Schrader, Slocum[148] recommended that only the minimum acetabular rotation necessary to maintain joint stability be performed (i.e. approximately 20°).

Complications following TPO are often related to alteration of the pelvic anatomy, excessive stress placed on the implants or both. The effect of various techniques on pelvic architecture and postoperative complications has been evaluated by several investigators [39, 56, 64, 120, 161, 162].

In a recent *in vitro* study, Graehler[39] analyzed the alteration of pelvic geometry following TPO. Transverse iliac osteotomies of varying angles, stabilized at 20°, 30° and 45° of acetabular ventroversion with either a 2.7 mm DCP or a pre-angled TPO plate (Slocum Enterprises, Eugene, Oregon) were evaluated. The author reported that severe lateralization of the acetabular segment and reduction of the pelvic inlet area occurred when the iliac osteotomy was oriented perpendicular to the axis of the ilium. Lateral displacement of the acetabular segment and pelvic narrowing were smallest with an osteotomy angled 20° to 30° from the axis of the ilium. Interestingly, this orientation corresponds to that recommended by Slocum[150] (i.e. normal to the long axis of the pelvis rather than ilium). Further lateralization of the acetabular segment and pelvic inlet narrowing were observed with increased acetabular ventroversion angles and with the use of twisted DCPs rather than pre-angled TPO plates. Considering the deleterious biomechanical effect of hip lateralization[3, 37] and the alteration of the pelvic architecture following TPO, Graehler recommended iliac osteotomy angles of 10° to 30° and the use of the smallest possible pre-angled TPO plate. Similar conclusions were drawn by Koch[64] who, in a retrospective radiographic study, compared 2 plating methods (twisted DCPs and pre-angled TPO plates). Koch concluded that due to the higher coverage and better congruence achieved with TPO plates, these implants offer a clinical advantage over the DCPs. In Koch's as well as other clinical studies[55, 120], cranial screw loosening occurred in approximately 30% of the cases regardless of the plating method, thus representing the major implant related complication. According to Koch, the high incidence of screw loosening may be related to the relatively small size of the implant and to the weak holding power of juvenile bone. The need for early postoperative weight-bearing and the relative mobility of the sacroiliac joint in young animals have also been suggested as potential causes for screw loosening[56, 178]. However, the clinical relevance of this implant failure remains uncertain as neither bone healing nor long term hip stability are affected. Along with the previously mentioned complications, sciatic nerve injuries, temporary constipation and/or dysuria (secondary to pelvic narrowing) have been occasionally reported[120, 150]. Pelvic narrowing can be limited by complete ostectomy of the acetabular branch of the pubis as dorsal and medial as possible[161, 162].

The postoperative results following TPO have been evaluated by several authors[82, 83, 140, 147]. In a 7-year retrospective study[147] involving 119 dogs, all dogs were subjectively described as having normal limb function and activity. Furthermore, no progression of degenerative joint disease was reported. In an other study[83], clinical lameness following TPO was resolved in 92% of the operated limbs. However, progression of osteoarthrosis, although limited, did occur during the 6 months follow-up period. Similar results have been reported by Schrader[140] who claimed 93% of satisfactory limb function despite limited range of motion, persistence of gait abnormalities, and crepitation in most postoperative instances. The effect of TPO on limb function has been objectively evaluated using force plate analysis. Recently, McLaughlin[83] demonstrated that the ground reaction force of dysplastic limbs after TPO reached normal values within 28 weeks and was significantly greater than the ground reaction force of untreated limbs. Moreover, the author reported that following TPO, hip congruity improved clinically and radiographically while congruence deteriorated in untreated hips.

DETERMINATION OF HIP CONTACT AREAS

During loading of a joint, articular cartilage is subjected to high contact stresses[110]. Alterations of stress magnitude, distribution pattern, or both, are believed to be responsible for cumulative tissue damage and osteoarthrosis[87, 119]. In an effort to better understand the mechanics of load distribution on articular cartilage, numerous methods have been proposed to quantify joint contact areas[4, 38, 48, 115, 144, 176].

Radiographic and sectioning techniques

The earliest investigations of joint contact were performed radiographically[81, 158]. More recently, assuming that the femoral head was spherical, Hefti[48] developed a method for the measurement of contact area between acetabulum and femoral head from frontal radiographs. A 2-dimensional template using polar coordinates as meridians and latitudes was divided in quadrangular segments (elementary surfaces of known dimensions). The template was centered on the femoral head on the patient's anteroposterior radiographs. The area covered by the acetabulum was inferred from the projected shadows of the acetabulum on the template, then by summation of the elementary surfaces. The contact area was obtained by subtracting the area of the acetabular fossa (estimated at 25% of the acetabular surface). According to Hefti, the technique lacks precision, in part, because of the difficulty of controlling radiographic magnification and the crude estimate of the surface of the acetabular fossa from anatomical data. However, the method has the merit of allowing rapid estimate of hip contact areas in clinical situations.

Computerized tomography (CT) with 3-dimensional reconstruction has improved the accuracy of radiographic techniques. Investigating hip coverage and congruency, Klaue[63] used sequential cross sectional CT images of the hip joint. An outline of the acetabular cartilage (representing articular contact) was drawn on each of the CT images. Then, the area of contact between articular surfaces was obtained by integration of the successive acetabular contours in the anteroposterior direction. Using this technique, Klaue determined that coverage of normal and dysplastic human hips respectively varied from 70% to 30% of the corresponding femoral head cross-section area. In this *in vivo* technique, hip joints were unloaded and contact was assumed to exist wherever acetabular cartilage was present. A similar method was described by Murphy[92] who modeled the acetabulum as a portion of a globe limited by the acetabular rim. Using 3-D reconstructed images Murphy predicted the effect of corrective procedures on hip containment. Contact was defined when opposite surfaces fell within a certain proximity to one an other.

Sectioning techniques have also been used to determine contact areas. Wiberg[174] analyzed femoropatellar contact from frozen sections. In an other study[145], contact was determined from sequential histological slabs from loaded joints. However, sectioning techniques are destructive and only one joint position can be evaluated for each specimen.

Dye staining techniques

With dye staining procedures, loaded joints are immersed into a dye solution (e.g. safranin or ferric ammonium) which diffuses between the articular surfaces, thus staining the non-contact areas[38, 40, 41, 176]. Once the load is removed, mapping of the contact areas is obtained using various techniques. Photographs, mesh grids, or calibrated paper templates have been used to highlight the contour of the contact area. Then digitalization, square enumeration, or orthogonal/polar coordinate graph techniques are used to measure contact areas. An advantage of dye staining techniques is that the staining dye can be neutralized for evaluation of the joint in various positions.

Casting techniques

In this method, a fast curing silicone rubber is injected, while still in a liquid phase, into a joint prior to load application. As load is applied, the silicone is squeezed out of the regions of contact, thus leaving holes in the solidified cast. Area measurement is performed in a manner similar to that used in the staining techniques[1, 115, 160, 177] or, as proposed by White[176], using a weight comparison technique.

Recently, Yao[177] introduced the "3-S technique" where a silicone oil-carbon powder suspension is squeezed out of regions of contact between loaded joint surfaces. The very short time (0.45 sec) required to define contact with this method is comparable to physiological loading, thus the technique better reflects the actual contact occurring during gait. Moreover, the procedure can be repeated under different loading conditions.

Pressure measurement techniques

In addition to measuring contact areas, pressure sensitive films are used to record contact pressure in joints[4, 45, 132, 146]. The films are made of two polyester sheets which, when pressed against each other, produce a red stain. A calibration procedure is required to assess the actual pressure from the intensity of the stain[91, 146]. Because of its simplicity, the pressure sensitive film technique has been used extensively in both *in vitro*[4, 19, 45, 154] and *in vivo* studies[132]. However, because the thickness and stiffness of the film prevent precise conforming to curved surfaces and promote movement between the polyester sheets, the use of this technique in complex joints is unsatisfactory[160].

Surface proximity techniques - Stereophotogrammetry

A method to evaluate joint contact, based on the calculation of the relative proximity of joint surfaces, was introduced by Sherrer[144]. The stereophotogrammetric method (SPG) combines mathematical modeling of the articular surfaces and kinematic analysis to reproduce *in vivo* joint alignment and calculate the distance between joint surfaces. The regions of opposing surfaces which fall within a prescribed distance from each other are defined as contact areas[91]. With SPG, the geometry of the articular surface is represented as a 3-dimensional mesh diagram. Equidistant regions are displayed as gray zones with intensity varying with the proximity of the opposing surfaces. This sophisticated technique has been used to determine both contact areas and cartilage thickness[4, 66, 154].

The relative merits of these methods have been investigated[4, 154, 160, 176]. Comparing dye staining, rubber casting, pressure film and SPG techniques, Ateshian[4] showed that dye staining consistently over-estimated contact areas because the surface tension of the dye solution precluded its diffusion in narrow gaps. Furthermore, the dye could not stain "islands" of non-contact areas. Conversely, the rubber casting method underestimated contact areas because the viscous silicone gel tended to remain as a thin film within the contact regions. Similarly, due to the threshold value of pressure sensitive films, this technique tended to underestimate contact areas as well. Furthermore, pressure films tended to shift inside of the joint which in turn could have altered the contact patterns. Nevertheless, contact areas determined by pressure films were most consistent with those obtained with SPG. Because stereophotogrammetry consistently showed contact in the same regions common to all techniques, Ateshian concluded that SPG was more accurate and reliable than casting and staining techniques especially in congruent joints[4].

In a study comparing staining, casting, and pressure film techniques, Stormont[160] underscored the difficulty of using pressure film in spherical joints and the tediousness of staining techniques. In contrast to Ateshian, Stormont reported that casting methods tend to over-estimate surfaces because of the "meniscus effect" around the edge of the contact areas. Stormont concluded that silicone casting was the most reproducible and reliable method. However, for White[176], both dye and casting techniques yield inaccurate results because tracing of curved 3-dimensional contours is made on flat surfaces.

In the survey presented in this thesis, the discrepancy between human and veterinary literature is apparent. While the biomechanics and treatment of congenital hip dislocation have been thoroughly investigated in human orthopaedics, emphasis has been placed on the investigation of the etiology and eradication of the disease in veterinary medicine. Furthermore, despite few theoretical studies in which the specifics of quadrupedal gait are considered, most of our knowledge about the biomechanics and treatment of hip dysplasia is extrapolated from the human literature. It is hoped that the current study will bring some objective new information about the rationale for the treatment of acetabular dysplasia in dogs.

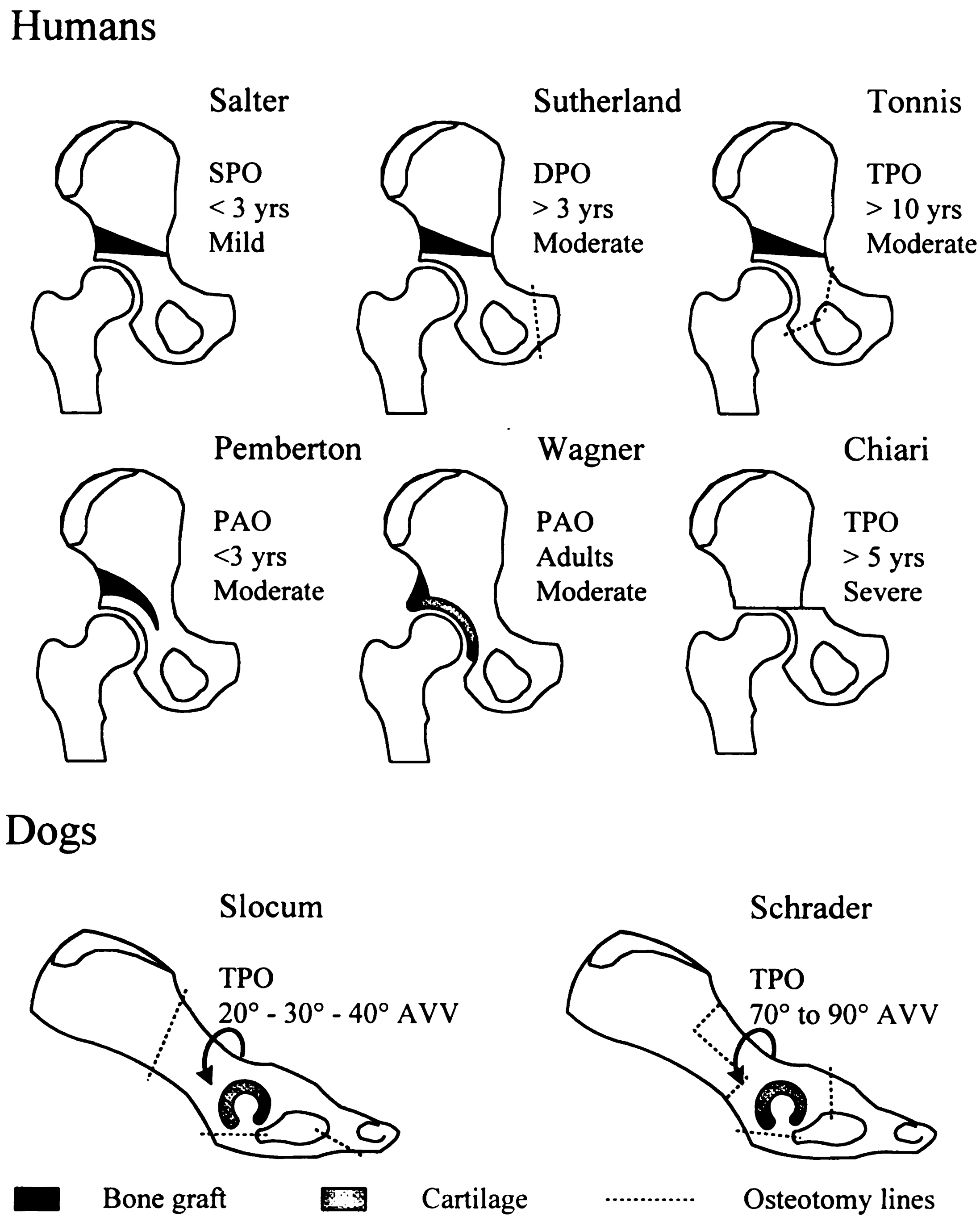

Figure S3 - Synopsis of the major pelvic ostetomies performed in humans and dogs. SPO, DPO, TPO and PAO = single, double, triple and periarticular pelvic osteotomy respectively. Indications with respect to age and extend of acetabular dysplasia are reported for human procedures. Potential amplitudes of acetabular ventroversion (AVV) are reported for veterinary procedures.

MATERIALS AND METHODS

This chapter provides a general description of the methodology followed in this study. Specimen selection criteria, specimen preparation, and surgical procedures being common to all aspects of the project are reported initially. When appropriate, the specific techniques and methods used to collect and analyze the data are described separately.

KINETIC STUDY

Specimen selection criteria

Three 8 month-old Labrador retrievers, diagnosed with hip dysplasia from routine ventrodorsal radiographs and a positive Ortolani sign were used in the study (Figure M1). To be considered, all dogs had to be potential candidates for TPO as defined in previous studies[139, 147]. The selection criteria included a normal femoral neck angle[133], appropriate acetabular depth, and absent or limited osteoarthrosis. All dogs had been euthanatized for unrelated reasons. Only 5 of the 6 hip joints were evaluated due to early remodeling of one acetabulum.

Figure M1 - Ventrodorsal radiograph of the pelvis and femurs from one of the dogs used in this study. Both hips are subluxated and there is minimal remodeling of the joints.

Model

The forces acting about the hip joint were evaluated using a previously described 2-dimensional mathematical model by Arnoczky and Torzilli[3] derived from anatomic radiographs in the frontal plane. Applying classic principles of static mechanical analysis, the model was based on anatomic muscle insertions and hip joint position to obtain the required angles and lever arms, thus allowing computation of the forces acting about the hip (Figure M2). While forces acting in the sagittal plane do exist during locomotion, as flexors and extensors act, only the forces acting in the frontal plane (abduction/adduction) during 3-legged stance were considered in this static 2-dimensional model.

With this model, a state of mechanical equilibrium is achieved when the external forces acting on the pelvic frame are balanced by internal muscle forces. The external forces are the ground reaction force shown in figure M2 as a knee reaction force (F_k) and a gravitational force (F_o). A resisting moment (M_o) due to the twisting force of the axial musculature is applied at the level of the sacral vertebrae[3]. In humans, during single-legged stance, equilibrium is only possible if the weight-bearing foot is shifted medially under the center of gravity (Figure M3). With hip adduction, the vertical projection of partial body weight (F_o) passes through the point of contact of the foot with the ground and directly opposes the ground reaction force (F_k)[3]. Unlike humans, dogs are quadrupeds and as such, have the ability to exert a torque or moment (M_o) through the spine and thoracic limbs (Figures M2 and M4). This moment acts in conjunction with the force generated by the abductor muscles (F_a) to keep the pelvis level[3].

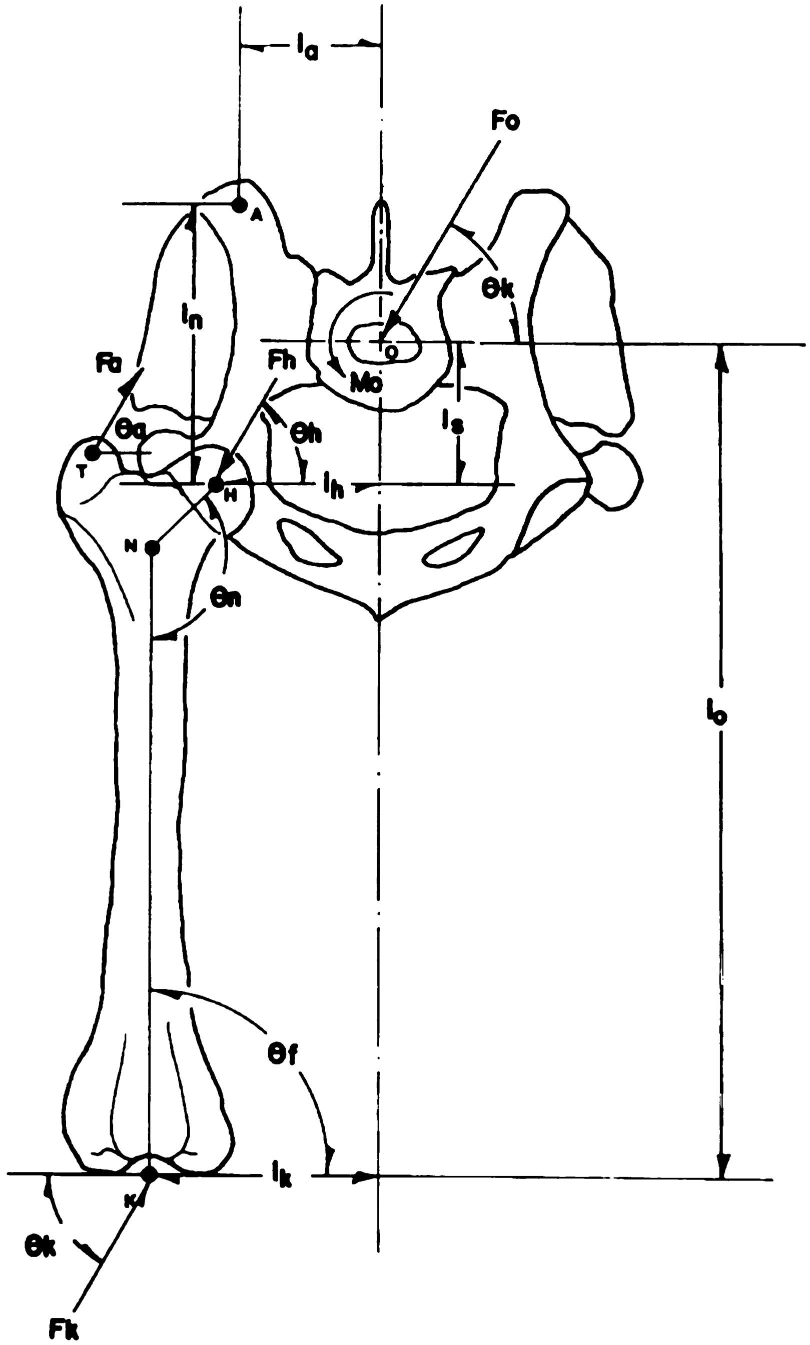

Figure M2 - Tracing of a radiograph illustrating measurements of lengths and angles used in computing the forces about the hip. These geometric parameters were obtained from pre- and postoperative radiographs (from Arnoczky[3], reproduced with permission).

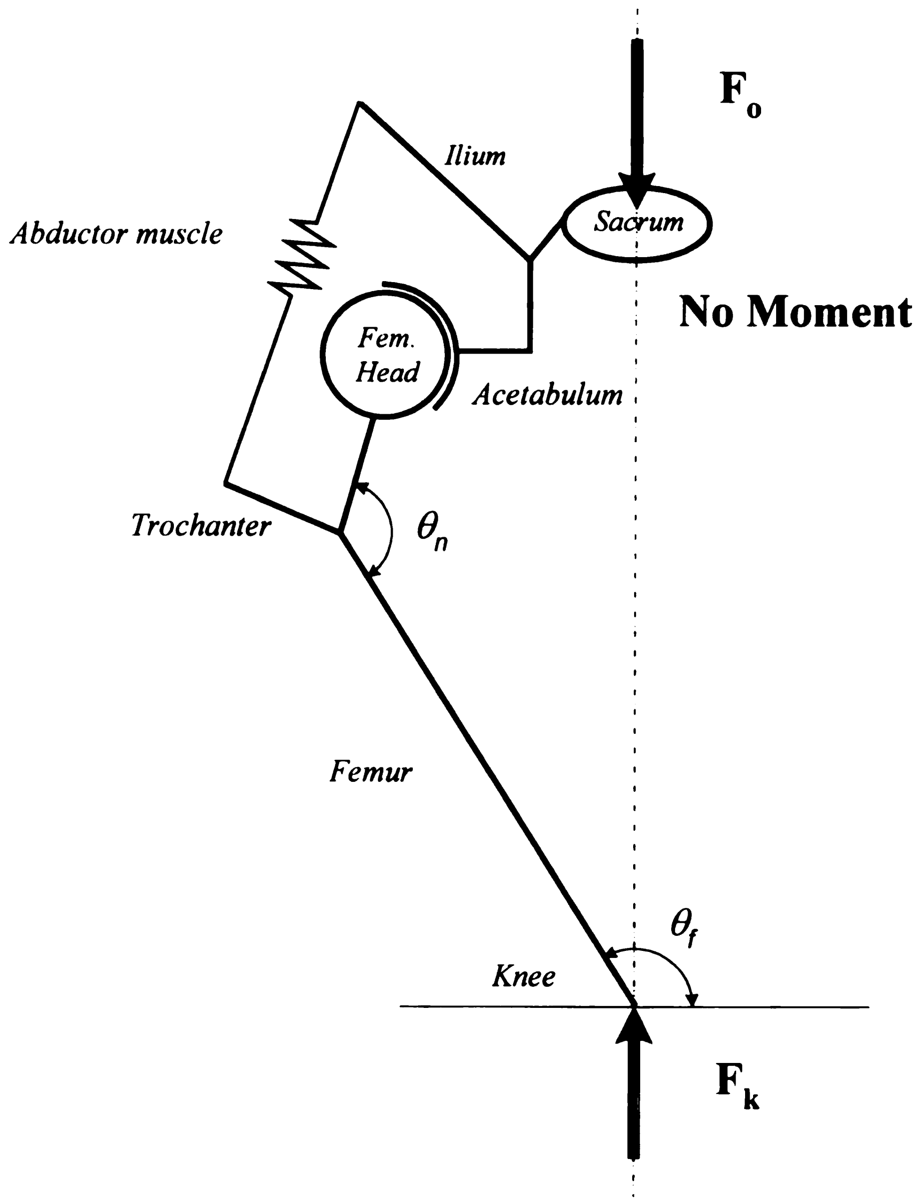

Figure M3 - Line drawing representing femur and pelvis with the femur in adduction. When the foot and the CG are aligned, no spinal moment exists. θn = femoral neck angle, θf = angle abduction, Fk = ground reaction force at the knee, Fo = gravitational force.

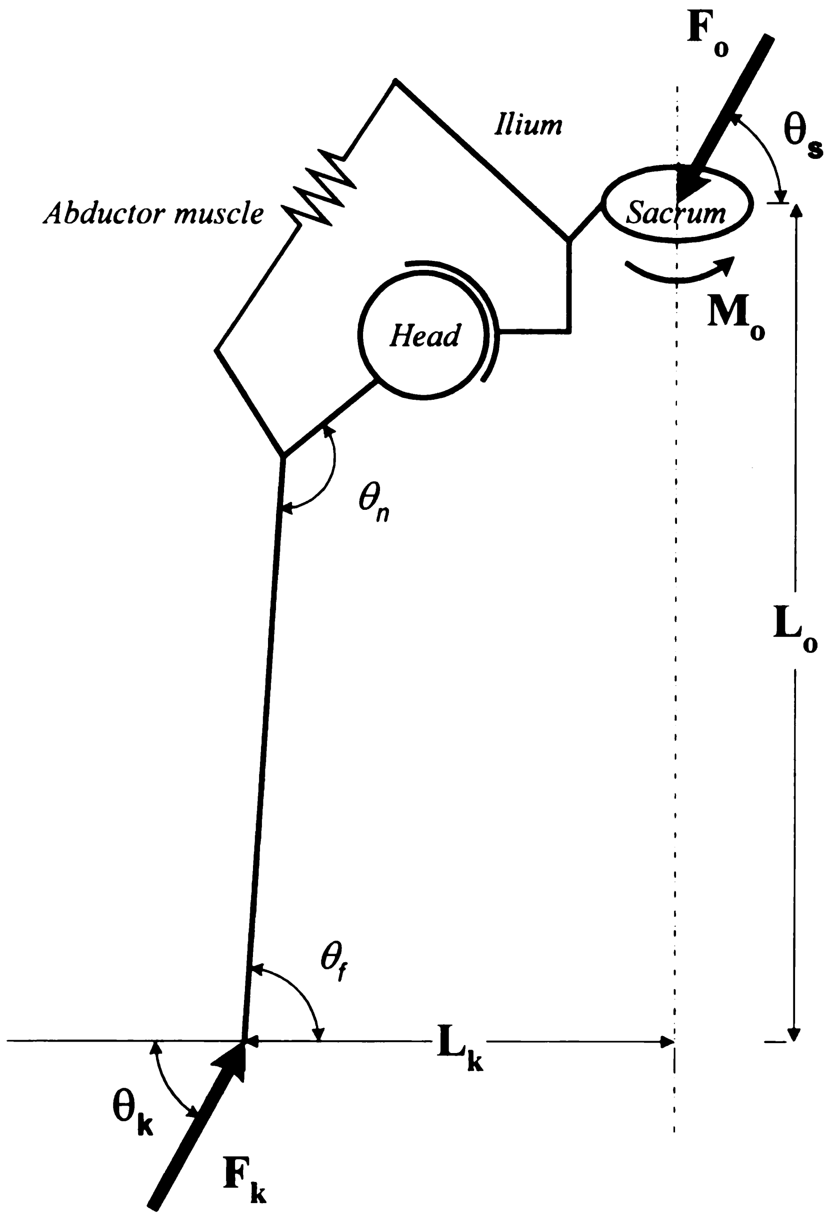

Figure M4 - Line drawing representing femur and pelvis with the femur in abduction. During 3-legged stance, abduction of the leg results in a moment Mo exerted on the spine. θn = femoral neck angle, θf = angle of abduction/adduction, Fk = ground reaction force at the knee, Fo = gravitational force.

In the 3-legged stance, the distribution of the body weight is not symmetric. Thus, the individual ground reaction forces are not equal and do not act strictly along the vertical. As a horizontal component exists, the force F_o must also act at an angle θ_s as shown in figure M4. From the free body diagram in figure M4, in a state of equilibrium the following equations have to be satisfied:

$$\Sigma Fx = F_k \cos\theta_k - F_o \cos\theta_s = 0 \quad (1)$$

$$\Sigma Fy = F_k \sin\theta_k - F_o \sin\theta_s = 0 \quad (2)$$

$$\therefore \quad F_k = F_o \quad (3)$$

and

$$\theta_s = \theta_k \quad (4)$$

Furthermore,

$$\Sigma M_{knee} = (F_o \cos\theta_k)\, L_o - (F_o \sin\theta_k)\, L_k + M_o = 0 \quad (5)$$

$$\therefore \quad M_o = F_o\,(L_k \sin\theta_k - L_o \cos\theta_k) \quad (6)$$

The free body diagram shown in figure M5 illustrates the forces and moment acting upon the pelvis, namely: the gravitational force F_o, the hip reaction force F_h, the abductor muscle force F_a and the spinal moment M_o. Considering a state of equilibrium, the following equations are inferred:

$$\Sigma Fx = 0 \;\therefore\quad F_h = (F_o \cos\theta_k + F_a \cos\theta_a) / \cos\theta_h \quad (7)$$

$$\Sigma Fy = 0 \;\therefore\quad F_h = (F_o \sin\theta_k + F_a \sin\theta_a) / \sin\theta_h \quad (8)$$

$$\Sigma M_{hip} = 0 \;\therefore\quad F_o\, L_s \cos\theta_k - F_o\, L_h \sin\theta_k - F_a\,(L_h - L_a) \sin\theta_a$$
$$+ F_a\, L_n \cos\theta_a + M_o = 0 \quad (9)$$

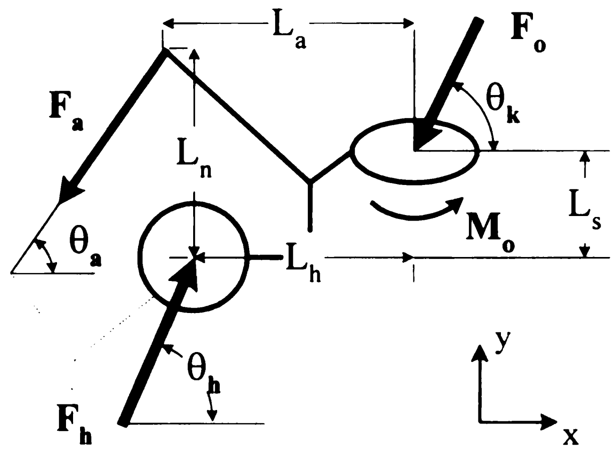

Figure M5 - Free body diagram representing forces and moment acting upon the pelvis in the frontal plane. See text for detail (equations 7 to 9).

Replacing M_o by (6) in (9) the following equalities are inferred:

$$F_a = \alpha F_o \tag{10}$$

where

$$\alpha = \{(L_o - L_s)\cos\theta_k + (L_h - L_k)\sin\theta_k\} \\ / \{(L_a - L_h)\sin\theta_a + L_n\cos\theta_a\} \tag{11}$$

The hip reaction force acts at an angle θ_h given by:

$$\tan\theta_h = (\sin\theta_k + \alpha\sin\theta_a) / (\cos\theta_k + \alpha\cos\theta_a) \tag{12}$$

where θ_a, determined by hip joint geometry, represents the angle of application of F_a.

The pelvic moment M_o, hip reaction force F_h, its angle of application θ_h and the abductor muscle force F_a are determined from equations 1 to 12 and the geometric length measurements of the canine skeleton obtained from cranio-caudal radiographs[3].

Although the exact magnitude of F_o is unknown, it has been hypothesized that, in a 3-legged stance, F_o corresponds to approximately a third of the body weight[3, 114]. This approximation has been confirmed by kinetic data[20]. While the angle of application of F_o is also unknown, it can be estimated from physical constraints and kinetic data. From the free body diagram in figure M4, it is assumed that the line of action of F_k must pass medially to the center of the hip. Indeed, with F_k passing laterally to the hip, F_k and F_o would generate a couple, which could not be realistically counteracted by M_o alone. Furthermore, it has been determined that the ground reaction force F_k possesses an horizontal component in the sagittal plane[20]. In order to satisfy these constraints, θ_k would approximately range between 50° and 80°. In this study, the angle θ_k which represents the orientation of both F_k and F_o (equation 4) was arbitrarily chosen at 65° with respect to the horizontal. Mechanical equilibrium is achieved when external forces are balanced by internal muscle forces. To keep the pelvis level, the abductor musculature must generate a force F_a which, in addition to M_o, counteracts the effect of F_o[3, 87]. The resultant of these external and internal forces is opposed by the hip reaction force F_h[3, 105, 109]. The forces acting about the hip, F_a and F_h, have been shown to vary in intensity and direction depending on the anatomical configuration and relationship of the joint[3].

<u>Specimen preparation</u>

The pelves and femurs were dissected *en bloc* and all soft tissues, except the joint capsules were removed. Care was taken to maintain the integrity of the joint capsules to prevent loss of synovial fluid. Specimens were frozen at -20°C until testing, then thawed at room temperature. Soft tissues were kept moist by spraying isotonic saline throughout the experiment. To obtain necessary geometric parameters and verify proper positioning, radiopaque markers were implanted symmetrically in each pelvis at the level of the iliac crests and sacral promontory, and in the femora at the insertion site of the gluteal musculature on the greater trochanters.

Experimental procedure

Specimens were placed on a specially designed radiolucent frame (Figure M6) which allowed the pelvis to be oriented in the functional position of a standing dog (40° of pelvic inclination[6], 110° of hip flexion[35], 5° of hip abduction[105]). Specimens rested only on the iliac wings and femora, thus allowing for unrestricted coxofemoral subluxation. Pre-operative radiographs were made in a craniocaudal orientation (Figure M7), then TPO was performed bilaterally following a previously reported procedure[148]. The long axis of the pelvis was determined by drawing a line from the ventral 1/3 of the ilium to the dorsal aspect of the ischiatic tuberosity. Using an oscillating bone saw, the acetabular branch of the pubis was ostectomized. A second osteotomy was performed through the ischial table along the lateral limit of the obturator foramen. The iliac osteotomy was made perpendicular to the axis of the pelvis and caudal to the sacrum (Figure M8). Pre-angled plates (Slocum Enterprises, Eugene, OR) were used to achieve accurate acetabular ventroversion (Figure M9). Three angles of AVV (20°, 30° and 40°) were successively studied in each specimen. Radiographs were repeated after each procedure (Figure M10).

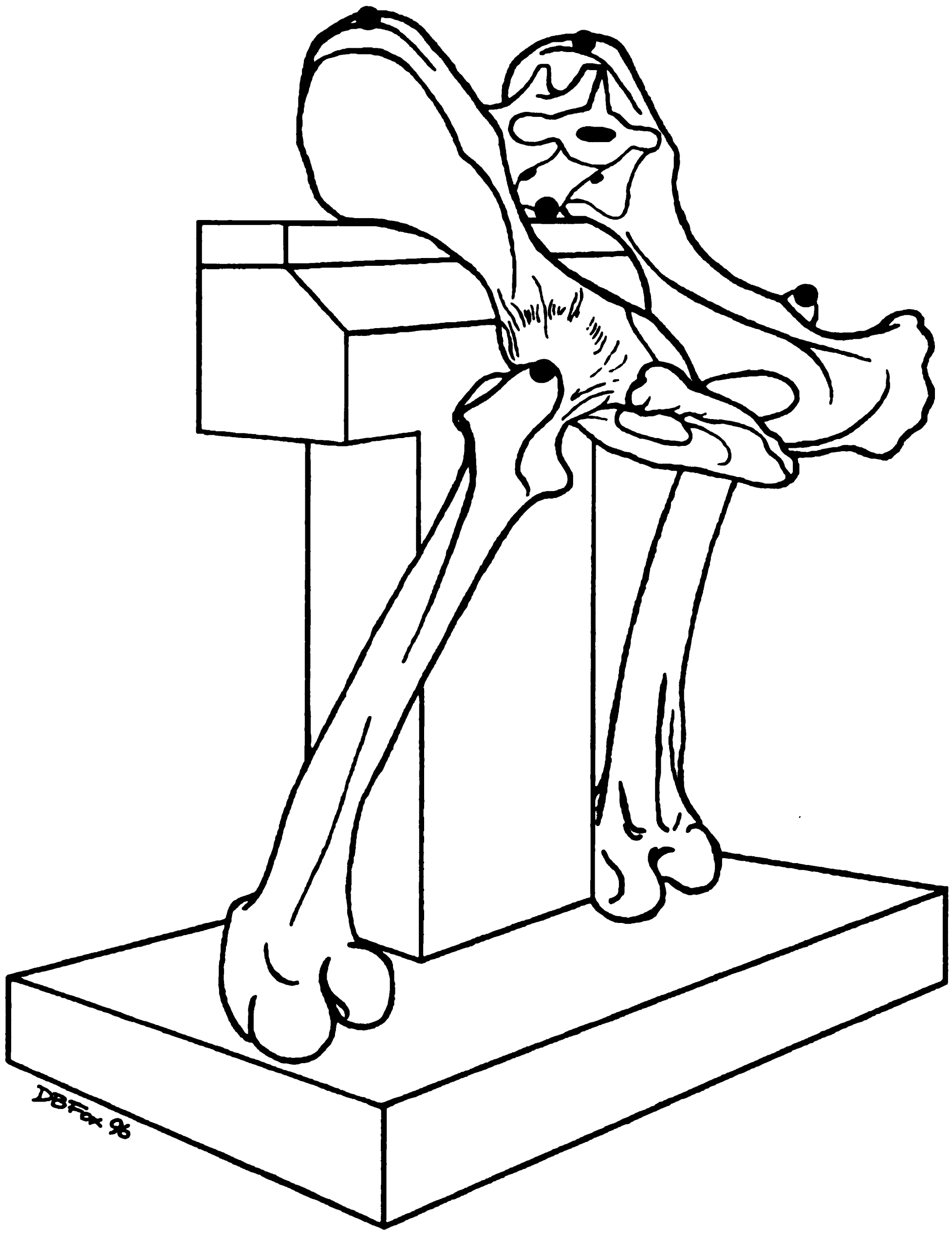

Figure M6 - Drawing of the radiolucent frame with specimen oriented in the functional position of a standing dog (40° of pelvic inclination, 110° of hip flexion, 5° of hip abduction). Wedges were used to maintain these angles consistent between dogs.

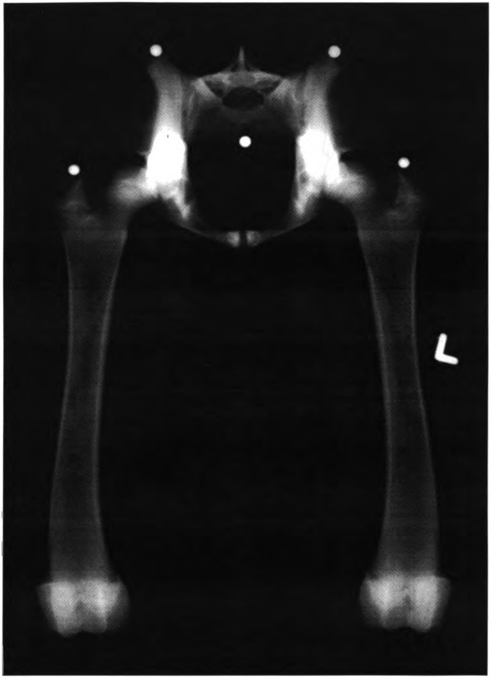

Figure M7 - Preoperative craniocaudal radiograph of the same pelvis as in Figure M1. Radiopaque markers have been implanted into the pelvis and femurs to obtain the required geometric parameters and to verify positioning. Both joints are subluxated.

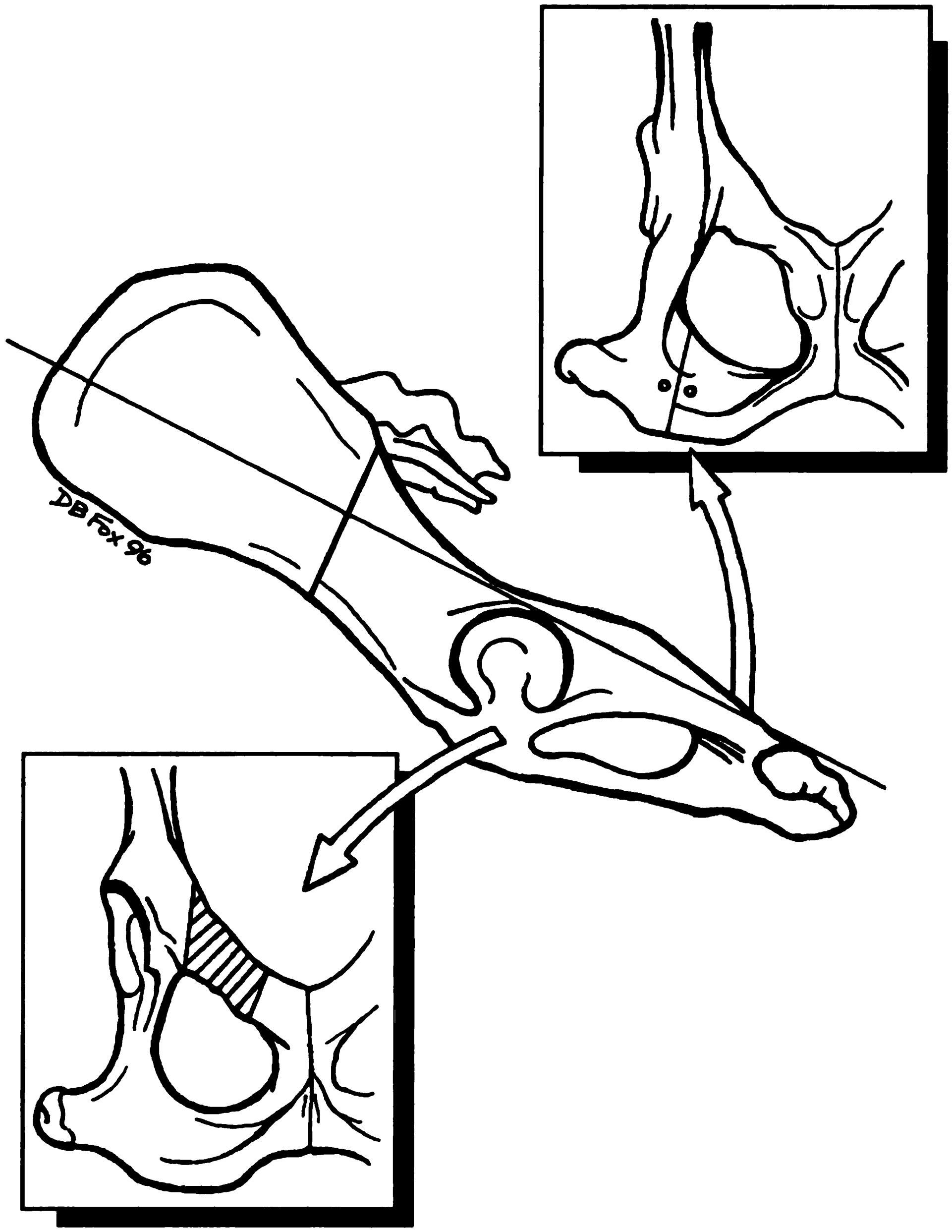

Figure M8 - Line drawing illustrating location and orientation of pelvic osteotomies according to the procedure described by Slocum[148].

Figure M9 - Photograph of the pre-angled TPO plates. Three angles are currently available: 20°, 30° and 40°. These plates are lateralized for right and left procedures.

Figure M10 - Postoperative craniocaudal radiograph showing 20° of acetabular ventroversion. The right hip is relocated while the left hip remains subluxated.

Data collection

Measurements relating to femoral and pelvic geometry, as well as coxofemoral relationship, were obtained from each radiograph using the template shown in figure M2. Using a custom-designed computer software[3], the hip reaction force (F_h) and the abductor muscle force (F_a) were determined. The resultant angles of application of these forces (θ_h and θ_a, respectively), with respect to the horizontal plane, were also computed (θ_h) or inferred from geometric measurements on the radiographs (θ_a). Forces were expressed as a function of the gravitational force (F_o) and their angles of application were reported in degrees.

Data analysis

Kolmogorov-Smirnov normality test was used to ascertain that the data was normally distributed. Homogeneity of variances was verified using Barllett's test. A two-factor analysis of variance (dog, angle of acetabular ventroversion) was used to evaluate the hip forces and angles of application as a function of acetabular ventroversion. Tukey's post-hoc test followed to locate significant differences (with values of $p < 0.05$).

ANATOMICAL STUDY

Specimen selection / preparation

Six young adult (age < 18 months) Labrador retrievers, diagnosed with hip dysplasia as determined from routine ventrodorsal radiographs, and a positive Ortolani sign were used in this study. The animals, similar in size and body weight (range: 61 lbs to 68 lbs) were selected following the same criteria as in the kinetic study. These included normal femoral neck angle, appropriate acetabular depth, and absence of osteoarthrosis as determined from preoperative radiographs. The Ortolani angles of reduction and luxation were recorded under anesthesia (Appendix A).

In addition, 5 young adult (age < 3 years) mongrel dogs free of hip dysplasia (as determined from normal radiographs and absence of an Ortolani sign) were used in this study. The dogs represented a wide range of body size and weight (30 lbs to 70 lbs). After euthanasia (for reasons unrelated to this study or musculoskeletal pathology), pelves and femurs were harvested, prepared and stored until testing as previously described.

Experimental procedure

Before testing, approximately 0.5 ml of synovial fluid was removed from the joints and replaced with 0.5 ml of hydrosoluble contrast medium Hypaque® 60% (Sanofi, New York, NY). The substitution of synovial fluid was performed to prevent artificial worsening of coxofemoral subluxation secondary to an increase in intra-articular volume[73, 74]. The hips were then manipulated to facilitate diffusion of the contrast medium throughout the joint. Each pelvic-femoral unit was then secured on a specially designed Plexiglas frame (Figure M11). Specimens were oriented in the functional position of a standing dog (long axis of the ilium at a 40° angle with the horizontal, hip flexion angle of 110° and abduction angle of 5°). In order to reproduce *in vivo* conditions, axial load (approximately 1/3 of the body weight) was applied to the hip joints using a custom designed loading device. This device was composed of a nylon threaded rod on which 2 strain gages had been affixed and an articulated loading bar which bridged the acetabuli and functioned as a universal joint (Figure M12). The rod passed through the bottom of the Plexiglas frame and the center of the acetabular loading bar (Figure M13). Tension was controlled by tightening wing nuts at either end of the rod. Load was monitored via the strain gages throughout the experiment (Appendix B). In order to optimize joint contact, articular cartilage was allowed to creep for at least 15 minutes before data collection[5]. The frame/specimen complex was then inverted and introduced in the gantry of a CT scanner (Figure M14). This positioning allowed the contrast medium to flow by gravity to the dorsal aspect of the joint where articular contact occurs. The higher concentration of contrast medium so obtained enhanced the difference between lines of contact (black) and filled joint spaces (bright white) and facilitated the interpretation of the scanned images. Positioning of the specimen was verified by aligning the laser guides of the CT scanner with landmarks etched on the Plexiglas frame. Preoperative serial CT scans of each specimen (normal and dysplastic) were then performed in the transverse plane.

A TPO was then performed bilaterally on the dysplastic specimens following the procedure previously described. Specially designed pre-angled TPO plates were used to achieve accurate ventroversion of the acetabulum. Three angles of rotation of the ilium and acetabulum were studied in each specimen (20°, 30° and 40°). Postoperative CT scans of the dysplastic specimens were repeated for each of the angle of acetabular ventroversion.

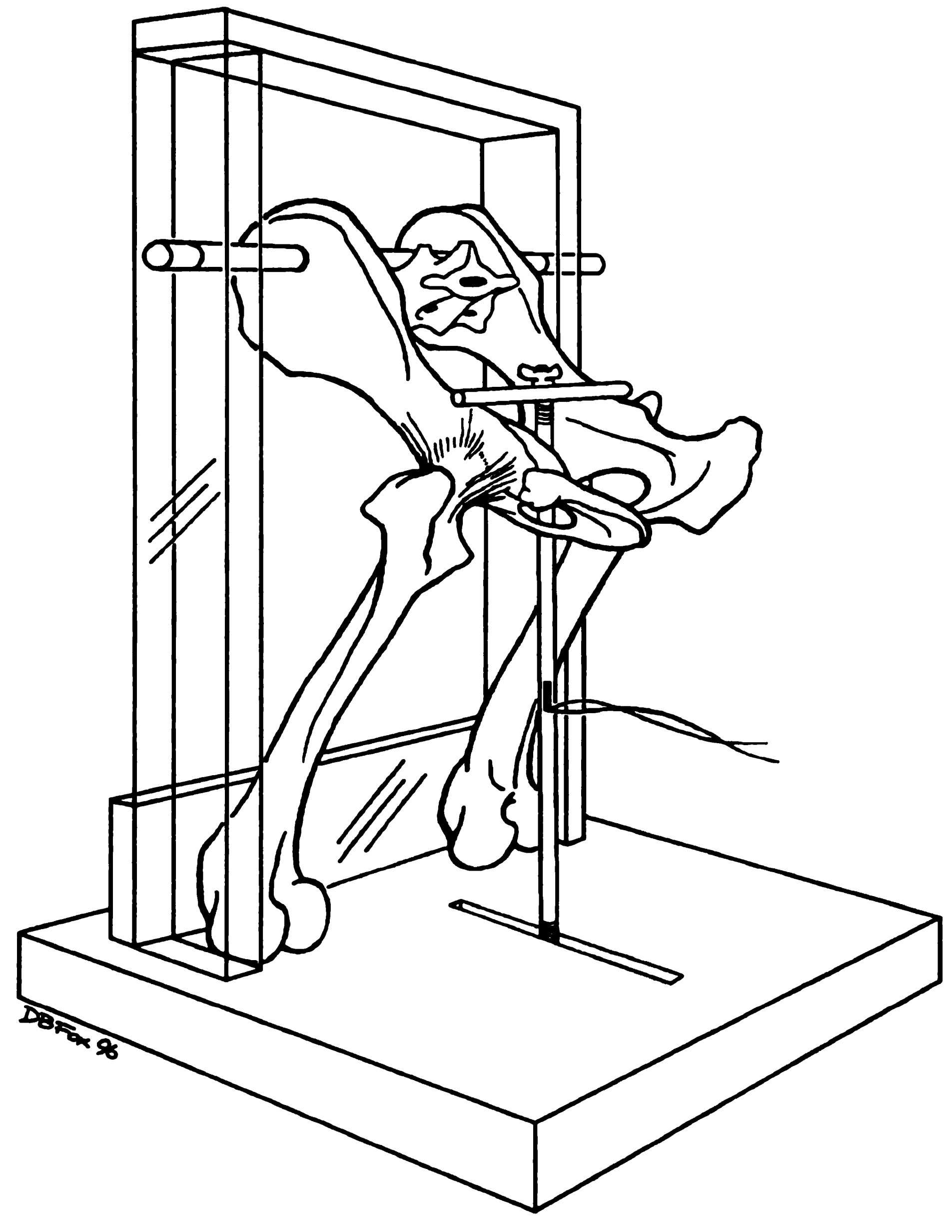

Figure M11 - Drawing of the custom design Plexiglas frame with specimen oriented in the functional position of a standing dog (40° of pelvic inclination, 110° of hip flexion and 5° of abduction).

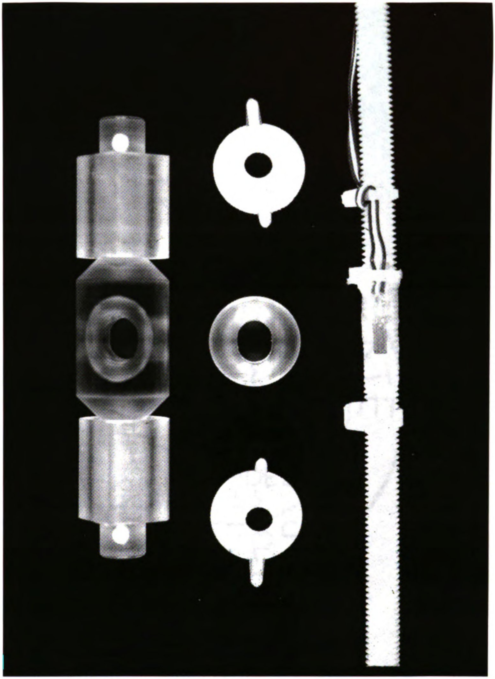

Figure M12 - Photograph of the custom designed loading device composed of a nylon threaded rod on which 2 strain gages have been affixed and an articulated loading bar which bridged the acetabuli and functioned as a universal joint.

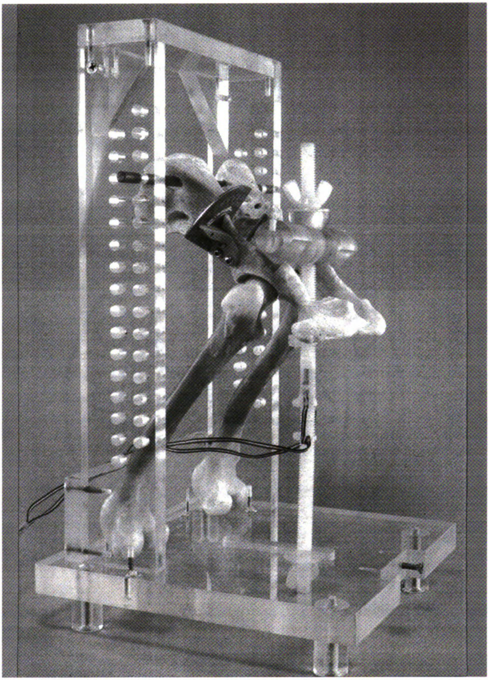

Figure M13 - Photograph of the custom designed frame with the loading device applied to a specimen. Loads (derived from strain gages) were read from the strain indicator. By controlling the tension applied to the nylon rod, a constant load equal to approximately 1/3 body weight was maintained throughout the experiment.

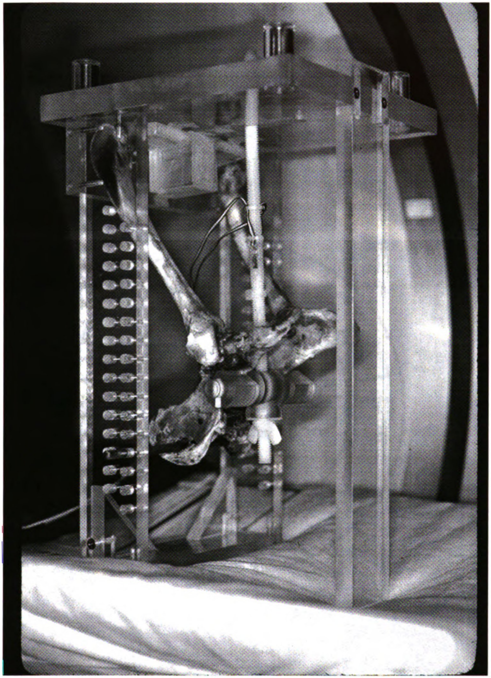

Figure M14 - Plexiglas frame with a specimen introduced in the gantry of the CT scanner. The inverted position facilitated diffusion of the contrast medium towards the dorsal aspect of the joint, thus improving the definition of the lines of articular contact on the CT scan images.

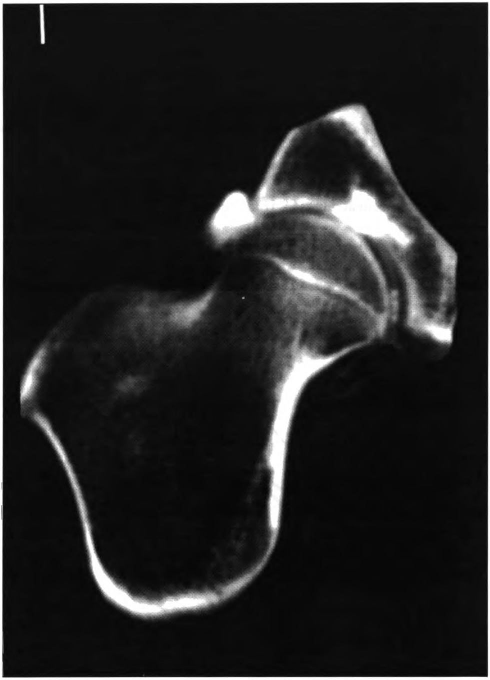

Figure M15 - Cross sectional CT scan image of a hip joint illustrating articular contact. Contact was defined by the absence of contrast medium between acetabulum and femoral head at any level free of intra-articular connective tissue (round ligament). The acetabular ventroversion angle is 20°. The section is located near the center of the head.

Data collection

The geometric parameters required for the computation of the contact areas were obtained from the CT cross sectional images. A magnification ratio of one was used throughout the experiment. Contact was defined by the absence of contrast medium between acetabulum and femoral head at any level free of intra-articular connective tissue, i.e. fat and round ligament (Figure M15). Measurement of the individual line of contact between acetabulum and femoral head was obtained from each successive cross sectional image. A "best fit" circle was centered on the femoral head and the line of contact was computed as an arc (A) of this circle (Figure M16).

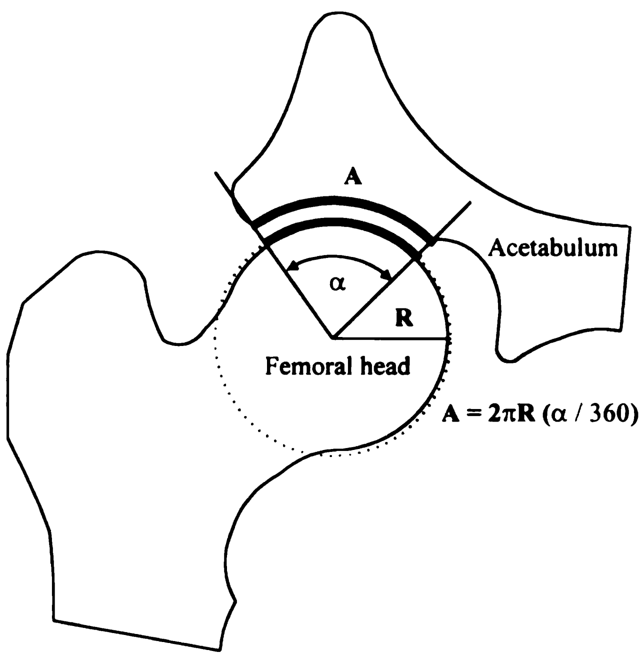

Figure M16 - Schematic of a cross section of a hip joint in the transverse plane. The femoral head is overlapped by a "best fit" circle (radius R). The bold arc corresponds to the line of contact between femoral head and acetabulum. The length of this arc (A) is a function of the angle α and is easily computed: $A = 2\pi R (\alpha/360)$.

The corresponding contact area, dS, was computed knowing the thickness, dX, of the scanner slices (1.5 mm) using dS = A (dX). Determination of the total joint contact surface (C) was made by summation of the individual contact areas (Figure M17). In order to make meaningful comparisons between dogs of different sizes, contact areas were expressed as a percentage of the femoral head surface. Assuming that the femoral head is almost spherical, the maximum potential contact area between acetabulum and femoral head (C_m) was arbitrarily defined as half the surface of a sphere having for diameter the maximum diameter of the head (D_m). Therefore, $C_m = \pi (D_m)^2 / 2$. As an example, if $D_m = 23$ mm, then $C_m = 831$ mm^2. The actual contact area $C = \Sigma$ dS was expressed as a percentage of the femoral head surface: $C\% = C / C_m$. Following this methodology, the areas of contact were measured preoperatively in one hip per normal and dysplastic specimen (the hip exhibiting the best contrast was chosen for calculation). The altered contact areas were computed postoperatively in the dysplastic dogs.

In addition, the angle of coverage of the femoral head by the acetabulum was determined. Coverage, which refers to the relationship between the acetabular lip and the hip reaction force, is best estimated by the center-edge angle[89]. This angle omega (ω) is similar to the Norberg[34] or Wiberg[173] angles and was defined by a line connecting the dorsal acetabular rim to the geometrical center of the femoral head and the horizontal passing by this center (Figure M18). The angle of coverage was measured preoperatively (normal and dysplastic dogs) and postoperatively (dysplastic dogs only) at the level of the maximum diameter of the femoral head.

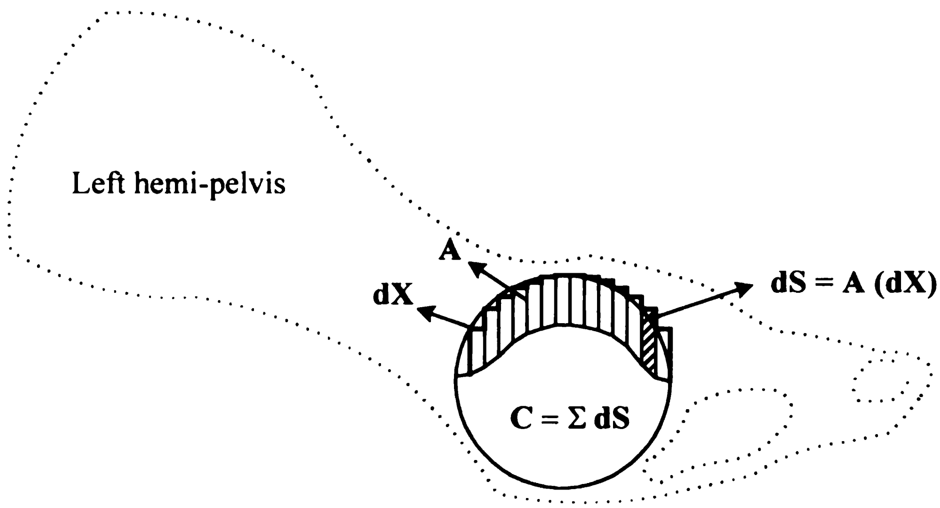

Figure M17 - Schematic of the lateral aspect of the femoral head. Each individual surface of contact (dS) is computed: dS = A (dX), where dX is the thickness of each CT scan slice (1.5 mm). The overall surface of contact, C, is obtained by the summation of the elementary surfaces: C = Σ dS.

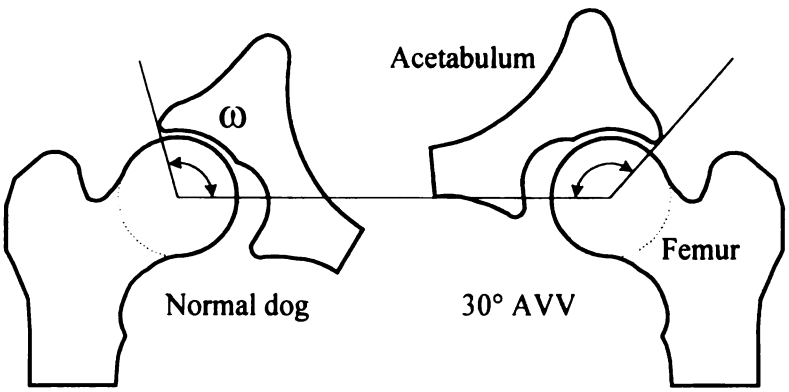

Figure M18 - Schematic of the hip joints in the transverse plane illustrating the angle of coverage ω.

Data analysis

Kolmogorov-Smirnov normality test ascertained the normal distribution of the data. Homogeneity of variances was verified using Barllett's test. A repeated measure ANOVA followed by Fisher least significant difference post-hoc test were used to evaluate changes in contact areas as a function of AVV. The significance level was set at $p < 0.05$. Contact areas between normal and subluxated dysplastic hips and between normal and dysplastic hips, once reduction had occurred, were compared using unpaired *t-tests*. The same procedure was used to compare angles of coverage between the groups. However, as 2 unpaired *t-tests* were used, the comparison-wise type 1 error rate was reduced to $p < 0.025$ in order to maintain an experimental-wise type 1 error at $p < 0.05$.

FUNCTIONAL STUDY

Evaluation of the experimental angles of reduction and luxation was performed immediately following data collection for the contact study. The same hips were evaluated in both experiments.

Experimental procedure

After completion of the anatomical study, the pre-angled TPO plates (20°, 30° or 40°) were replaced by a custom designed plate. This plate composed of two halves was designed to accommodate the screw holes of the TPO plates. A pivotal axis was built along the ventral aspect of the plate so that the two halves of the plate could rotate about each other. The plate therefore functioned like a hinge which allowed for continuous increase of the angle of acetabular ventroversion. The angles of reduction and luxation were recorded from a protractor mounted to the hinge plate (Figure M19). By design, the hinge plate provided a range of acetabular ventroversion extending from -10° (internally) to +45° (externally).

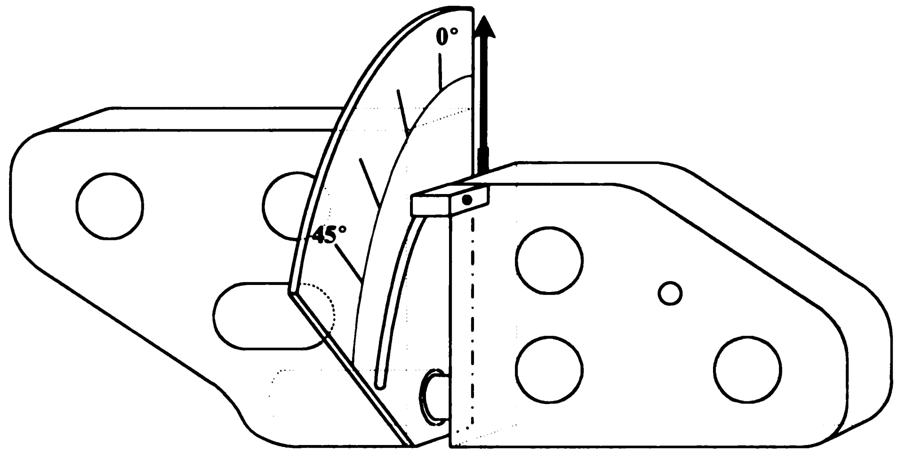

Figure M19 - Schematic of the custom designed hinge plate. The plate functioned like a hinge allowing for continuous increase of AVV. The range of motion extended from -10° to +45°. Angles of reduction and luxation were recorded from the protractor mounted to the plate.

Data collection

With the hinge plate affixed to the ilium, each specimen was repositioned in the Plexiglas frame as described earlier. A nominal compressive load was applied to the hip joints via the use of a rubber band which replaced the nylon rod of the loading device used in the contact study. Acetabular ventroversion was then gradually increased from 0° (subluxated position) until stable reduction of the femoral head occurred. The value of the angle of reduction was recorded from the protractor (Figure M20). The plate was then brought back towards 0° until the hip subluxated. The value of the angle of subluxation was also recorded. The procedure was performed bilaterally in all dysplastic specimens.

The ability to rotate the plate internally was an important feature because the ilium (upon which the plate is affixed) is slightly twisted in the caudomedial direction. Therefore when the hinge-plate was adjusted to the ilium **before** osteotomy, a negative angle of about 4° could be recorded. The pre-angled TPO plates are accurately set at 3 different angles (20°, 30°, 40°). These angles however are measured with respect to a neutral plane, **not** with respect to the anatomy of the ilium. Therefore, in order to compare the hinge plate and the TPO plate the following had to be considered:

1) the angle of acetabular ventroversion when using a TPO plate is actually greater than the pre-set angle (by whatever the anatomic medial tilt of the ilium is),

2) the angles of reduction / luxation determined by the use of the hinge-plate have to be measured with respect to a neutral plane, **not** in relation to the anatomy of the ilium.

The discrepancy between the actual angle of AVV and the "claimed" angle of AVV was ascertained in a separate radiographic evaluation (Appendix C).

Data analysis

A paired *t-test* was used to compare the previously recorded Ortolani angles and the experimentally measured angles of reduction and luxation. The strength of the correlation between the clinical (Ortolani) and experimental (hinge plate) methods was also evaluated using Pearson product moment linear correlation method. The significance level was set at $p < 0.05$.

Figure M20 - Photograph of the actual hinge plate applied to a specimen. Acetabular ventroversion was gradually increased from 0° (subluxated position) until stable reduction of the femoral head occurred. The value of the angle of reduction was recorded. Note that because the reference point is located at 40° on the protractor, the actual mark at 55° corresponds to 15° of AVV.

RESULTS

The results of each aspect of the study are presented with respect to their corresponding hypotheses.

KINETIC STUDY

Although no significant differences could be determined between right and left sides within each dog, some variation in the data inherent to anatomical diversity between dogs was observed. Numerical values of F_h, F_a, θ_h and θ_a as a function of acetabular ventroversion are reported at the end of this chapter in Tables R4 and R5.

In all specimens, reduction of the preoperative subluxation was consistently observed at 20° of acetabular ventroversion.

Magnitude of hip reaction and abductor muscle forces

The results of this study showed that the hip reaction force F_h was more than 2.8 times the gravitational force F_o in dysplastic hips. This is in contrast to a hip reaction force of approximately 2.6 inferred from Arnoczky's study in normal dogs[3]. Furthermore, in all 3 dogs evaluated in this part of the study, both the hip reaction force F_h and the abductor muscle force F_a showed a significant decrease from 0° (neutral position) to 20° of AVV (reduced position). Although this decrease continued from 20° to 30°, no significant difference could be detected. Both forces tended towards an asymptotic value between 30° and 40° (Figure R1). Data is summarized in Table R1.

Table R1 - Magnitude (mean ± sd) of the hip forces and corresponding angles of application for different angles of AVV. Significant differences (*, $p < 0.05$) were observed for all parameters between 0° and 20° of AVV. No significant differences were observed beyond 20° of AVV.

	ACETABULAR VENTROVERSION			
	0°	**20°**	**30°**	**40°**
$\mathbf{F_h/F_o}$	2.85 ± .24 (*)	2.47 ± .2	2.36 ± .18	2.36 ± .18
$\mathbf{F_a/F_o}$	1.86 ± .22 (*)	1.48 ± .2	1.36 ± .18	1.36 ± .18
θ_h	56.9° ± 2.9° (*)	60.1° ± 2.3°	60.8° ± 2.2°	60.8° ± 2.3°
θ_a	52.4° ± 4.9° (*)	56.6° ± 4.2°	57.5° ± 4.2°	57.5° ± 4.2°

Direction of hip reaction and abductor muscle forces

The decrease in the amplitude of the forces corresponded to an increase in their angle of application towards the vertical. The angle of application of the hip reaction force (θ_h) was approximately 56.9° in dysplastic hips which is substantially smaller than the 64° angle inferred from Arnoczky's study in normal dogs[3]. The changes in both θ_h and θ_a followed the same statistical trends as observed with the hip forces (Figure R2). Statistically significant decrease in the angles of application of the hip forces was found between 0° and 20° of acetabular ventroversion. The angle of application of the hip reaction force θ_h (mean ± sd), increased from 56.9° ± 2.9° to 60.1° ± 2.3° and 60.8° ± 2.2° as the angle of AVV changed from 0° to 20° to 30°. Similarly, the measured values of the angle of application of the abductor muscle force θ_a (mean ± sd) were 52.4° ± 4.9° preoperatively, then successively 56.6° ± 4.2° and 57.5° ± 4.2°. Both θ_h and θ_a remained virtually unchanged between 30° and 40° (60.8° ± 2.3° and 57.5° ± 4.2°, respectively). Data is summarized in Table R1.

Effect of Acetabular Ventroversion on Hip Force (F_h) and Abductor Muscle Force (F_a)

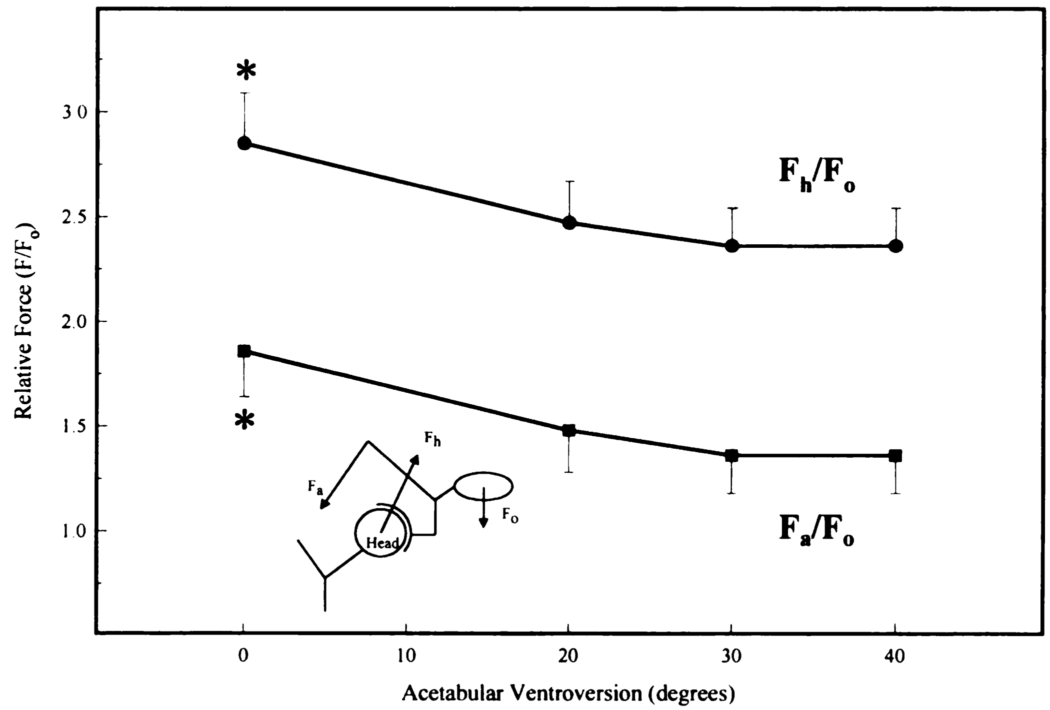

Figure R1 - Effect of the degree of acetabular ventroversion on the amplitude of the hip reaction force (F_h) and abductor muscle force (F_a). The forces F_h and F_a (mean ± sd) are expressed as a function of F_o. For general purposes, one can assume that F_o is equal to a third of body weight. Significant differences (*, $p < 0.05$) were only observed between 0° and 20° of acetabular ventroversion.

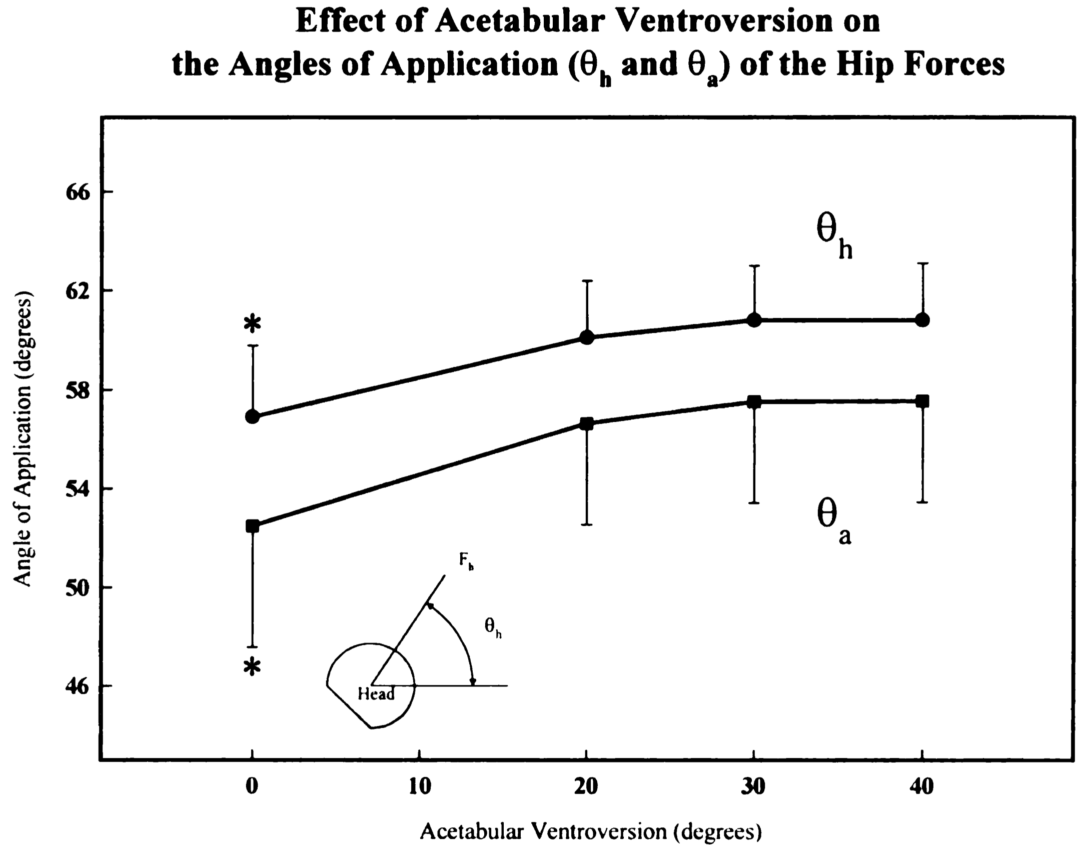

Figure R2 - Effect of the degree of acetabular ventroversion on the orientation of the hip reaction force (θ_h) and abductor muscle force (θ_a). The angles are reported in degrees. Significant differences (*, $p < 0.05$) were only observed between 0° and 20°of acetabular ventroversion.

ANATOMICAL STUDY

Contact areas

Contact areas (C) were expressed as a percentage (C%) of the femoral head surface (C_m) as follows: $C\% = C / C_m$. The femoral head surface C_m was arbitrarily defined as half the surface of a sphere having for diameter the maximum diameter (D_m) of the femoral head. Contact areas were measured preoperatively in one of the hips of each normal and dysplastic specimen. The altered contact areas were computed postoperatively in the dysplastic dogs only. Numerical values of the contact areas in normal dogs and, as a function of acetabular ventroversion in dysplastic dogs, are reported at the end of this chapter in Table R6. Summarized data is presented in Table R2.

Table R2 - Magnitude (mean ± sd) of the percentage of articular contact between femoral head and acetabulum and angles of coverage of the femoral head for different angles of AVV. Significant differences (*, $p < 0.05$) were observed for both parameters between 0° and 20°, 30°, and 40° of AVV. No significant differences were observed beyond 30° (contact) or 20° (coverage). Contact and coverage in normal dogs (**boldface**) were significantly different from those of dysplastic dogs.

	ACETABULAR VENTROVERSION				
	0°	**Normal**	20°	30°	40°
Contact (%)	4.3 ± 1.0 (*)	**17.4 ± 0.2** (*)	20.1 ± 0.8 (*)	21.1 ± 0.6	21.2 ± 0.6
Coverage (°)	62 ± 8.7 (*)	**99.2 ± 1.3** (*)	104.6 ± 1.9	115.8 ± 4.3	125.8 ± 5.1

The result of this study showed that the area of contact between the acetabulum and the femoral head was significantly smaller in dysplastic (subluxated) hip joints as compared to normal (congruent) hips. Furthermore, contact area significantly increased from the neutral position to 20° of AVV. This increase persisted slightly, although significantly, from 20° to 30° of acetabular ventroversion. Finally, contact areas tended towards an asymptotic value between 30° and 40° (Figure R3). Changes in contact area mimicked the trends observed in the kinetic study.

In addition, articular contact area in normal hips was compared to that of dysplastic joints (once reduction of the initial subluxation had occurred). Although of similar magnitude, the contact area of normal joints was significantly smaller than that of reduced dysplastic hips.

In all specimens evaluated in this study, reduction of the initial coxofemoral subluxation was achieved at 20° of acetabular ventroversion. This phenomenon was also observed in the kinetic study.

Effect of Acetabular Ventroversion on Articular Contact Area

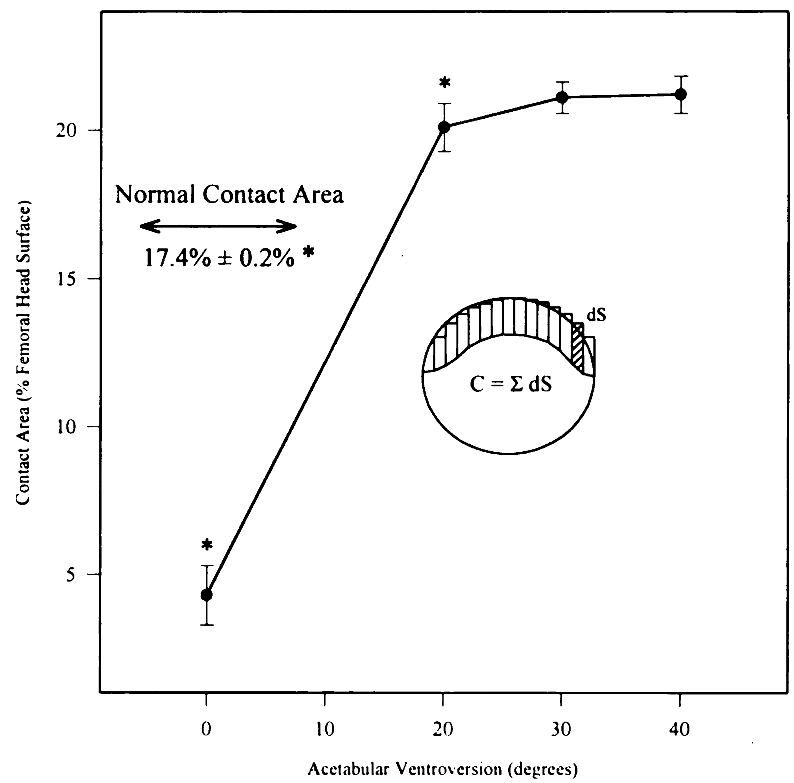

Figure R3 - Effect of the degree of acetabular ventroversion on articular contact between femoral head and acetabulum. Contact significantly increased (*, $p < 0.05$) from 0° to 20°, 30° and 40° of AVV. No significant differences were detected beyond 30°. Contact in normal dogs significantly differed from that of dysplastic dogs.

Acetabular coverage

Despite the large variety in size and body weight of the normal dogs, the angle of acetabular coverage, defined as the center-edge angle, was remarkably consistent (99.2° ± 1.3°) as shown by the very small standard deviation. This angle was significantly larger in normal congruent hips when compared to that of subluxated dysplastic hips. As acetabular ventroversion increased from 0° to 20°, coverage significantly increased from 62° ± 8.7° to 104.6° ± 1.9°. Beyond 20°, the increase in acetabular coverage occurred in approximately 10° increments which expectedly paralleled the increase in acetabular ventroversion (Figure R4). Numerical values of acetabular coverage in normal and dysplastic dogs are reported at the end of this chapter in Table R7. Data is summarized in Table R2.

The angles of acetabular coverage of normal and dysplastic hips (once reduction had occurred, i.e. at 20° of AVV) were compared. As observed with articular contact, coverage of normal hips was significantly smaller than that of reduced dysplastic joints.

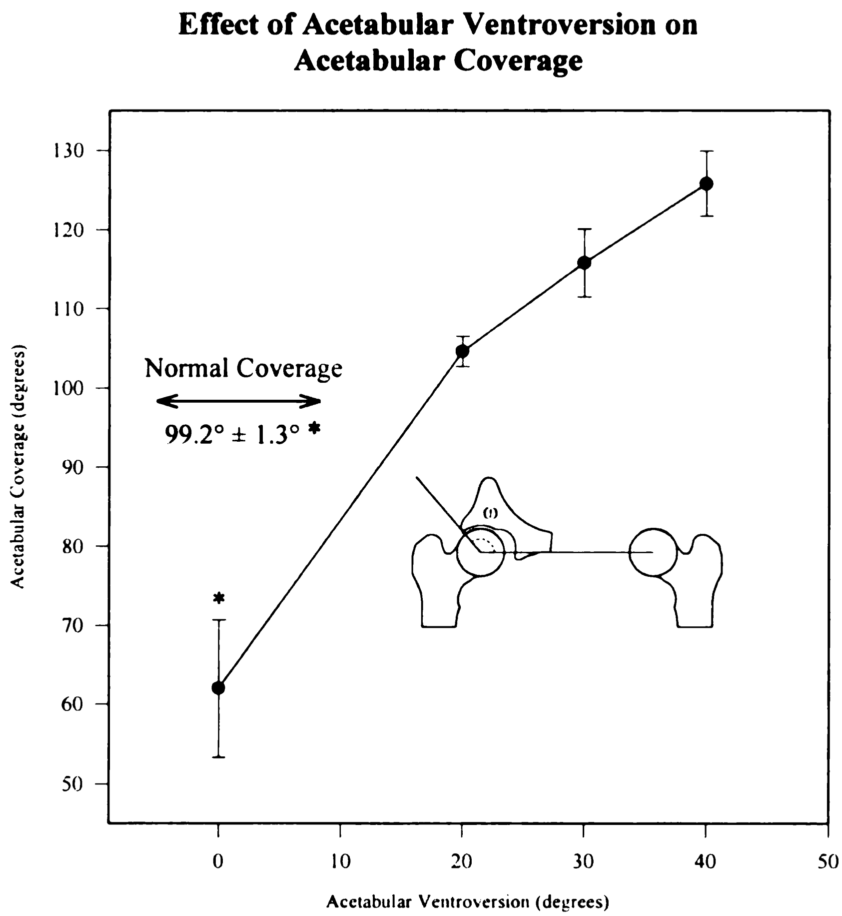

Figure R4 - Effect of the degree of acetabular ventroversion on acetabular coverage of the femoral head. Coverage significantly increased (*, $p < 0.05$) from 0° to 20° of AVV. Beyond 20°, coverage increased in 10° increments, paralleling the increase in AVV. Mean coverage in normal dogs significantly differed from that of dysplastic dogs.

FUNCTIONAL STUDY

As reported in the kinetic and anatomical studies, following TPO, reduction of the initial subluxation in dysplastic hips was consistently achieved at 20° of AVV.

Moreover, using the hinge plate, it was observed that reduction always occurred abruptly before 20° of AVV. The mean value of the angle of reduction for the dysplastic hips was 17.17° and the standard deviation was 1.33° (range 15° to 19°). The angle of subluxation ranged from 0° to 7° with a mean of 4.33° and a standard deviation of 3.01°. In comparison, the Ortolani angles of reduction and subluxation were 28.83° ± 3.82° (range 25° to 35°) and 4.83° ± 2.64° (range 0° to 8°) respectively. Data is summarized in Table R3.

As revealed by large p values, there was no significant correlation between angles of reduction or subluxation determined clinically (Ortolani) and their experimentally measured counterparts (hinge plate). Despite this lack of correlation, the Ortolani angle of reduction was significantly larger than the angle of reduction measured experimentally. There was no significant difference between the angles of subluxation.

For both normal and dysplastic dogs, numerical values of the contact areas, angles of coverage as well as angles of reduction and subluxation from both methods were recorded on individual data sheets (Appendix D).

Table R3 - Comparison between angles of reduction and luxation (mean ± sd) measured clinically (Ortolani) and experimentally (hinge plate).

	Reduction Angle	Luxation Angle
Ortolani	28.83° ± 3.82°	4.83° ± 2.64°
Hinge Plate	17.17° ± 1.33°	4.33° ± 3.01°
Correlation	p = 0.76 (NS)	p = 0.54 (NS)
Paired *t-test*	p = 0.00 (*)	p = 0.80 (NS)

Table R4 - Numerical values of the hip reaction force F_h and abductor muscle force F_a as a function of acetabular ventroversion.

	ACETABULAR VENTROVERSION							
	0°		20°		30°		40°	
	F_h/F_o	F_a/F_o	F_h/F_o	F_a/F_o	F_h/F_o	F_a/F_o	F_h/F_o	F_a/F_o
Dog # 1 (L)	2.72	1.74	2.4	1.4	2.3	1.3	2.3	1.3
Dog # 2 (L)	3.15	2.15	2.71	1.71	2.57	1.57	2.57	1.57
Dog # 2 (R)	3.06	2.06	2.66	1.66	2.53	1.54	2.53	1.54
Dog # 3 (L)	2.62	1.65	2.27	1.28	2.17	1.17	2.17	1.17
Dog # 3 (R)	2.69	1.72	2.33	1.35	2.22	1.23	2.22	1.23

Table R5 - Numerical values of the hip forces angles of application (θ_h and θ_a) as a function of acetabular ventroversion.

	ACETABULAR VENTROVERSION							
	0°		20°		30°		40°	
	θ_h	θ_a	θ_h	θ_a	θ_h	θ_a	θ_h	θ_a
Dog # 1 (L)	56.6	51.7	60.4	57.1	61.3	58.5	61.3	58.5
Dog # 2 (R)	61.4	59.8	63.4	62.5	64	63.3	64	63.3
Dog # 2 (L)	58	54.6	60.9	58.4	61.2	58.7	61.2	58.7
Dog # 3 (R)	54.9	48.8	58.4	53.3	59.4	54.7	59.7	55.2
Dog # 3 (L)	53.9	47.5	57.5	51.9	58.1	52.4	57.8	52

Table R6 - Numerical values of percentage of articular contact as a function of acetabular ventroversion. Normal values are also reported (**boldface**).

	ACETABULAR VENTROVERSION				
	0°	**Normal**	20°	30°	40°
	Contact Area in % of femoral head surface (C% = C/Cm)				
Dog #1	4.8	**17.4**	19.8	20.8	21.3
Dog #2	2.9	**17.5**	20.8	21.7	21.5
Dog #3	5.2	**17.3**	19.6	21.3	22.2
Dog #4	4.3	**17.7**	18.9	20.3	20.4
Dog #5	5.3	**17.2**	20.7	21.6	20.6
Dog #6	3.3	**NA**	20.9	21.0	21.0

Table R7 - Numerical values of the angle of acetabular coverage as a function of acetabular ventroversion. Normal values are also reported (**boldface**).

	ACETABULAR VENTROVERSION				
	0°	**Normal**	20°	30°	40°
	Acetabular Coverage				
Dog #1	70°	**98°**	103°	116°	125°
Dog #2	61°	**98°**	103°	112°	122°
Dog #3	72°	**100°**	107°	120°	130°
Dog #4	54°	**101°**	103°	112°	121°
Dog #5	65°	**99°**	107°	122°	134°
Dog #6	50°	**NA**	105°	113°	123°

DISCUSSION

Triple pelvic osteotomy (TPO) in dogs has been reported to resolve clinical lameness due to hip dysplasia in up to 92% of the affected limbs[83, 140, 148], (the percentage of spontaneous improvement of clinical lameness without surgery has yet to be determined). It has been hypothesized that clinical improvement following TPO results from increased femoral head coverage by the acetabulum[140, 148]. Suprisingly, although the correlation between articular stress and progression of osteoarthrosis has been well established[87, 119], no information was available on the effect of TPO on 1) the forces acting about dysplastic hip joints and 2) the actual area of articular contact of such hips. In the current study, the main alteration in the relationship of the coxofemoral joint due to TPO, was medialization of the femoral head resulting from the reduction of the initial subluxation. Increasing acetabular ventroversion (AVV) was thought to increase the tension on both the ventral joint capsule and the round ligament, thus pulling the femoral head into the acetabulum. As the edge of the dorsal acetabular rim moved beyond the geometrical center of the femoral head, the subluxated head abruptly relocated into the acetabulum. The initial relocation of the femoral head always occurred at an angle of AVV smaller than 20° and resulted in the most significant alteration in the magnitude of the hip reaction force (F_h). The smaller subsequent alterations of the configuration of the hip explains the more subtle changes in F_h observed between 20° and 40° of acetabular ventroversion. As the femoral head moves closer to the sagittal plane, the fulcrum effect of the gravitational force (F_o) is progressively reduced and consequently, maintenance of pelvic equilibrium requires less abductor muscle force (F_a)[87, 105, 109]. Because the lever arm of the abductors is virtually unchanged, the magnitude of F_a has to decrease as well. This, in, turn results in a decrease of the hip reaction force[87]. Indeed, the current study showed that the magnitude of F_h significantly decreased from more than 2.8 times F_o in subluxated hips to less than 2.5 times F_o after reduction. In the current study, the assumptions used in Arnoczky's original work were modified in order to encompass different physical and kinetic constraints. For instance, because of specimen positioning, the initial angle of abduction (θ_f) was 85°. Similarly, the angle of application of the gravitational force was arbitrarily chosen at 65° considering the existence of an horizontal component in the transverse plane. Interestingly, with these modified assumptions, the magnitude of F_h in reduced dysplastic hips was comparable to that of normal hips (approximately 2.6 times F_o) obtained from Arnoczky's original study[3].

Severe lateralization of the acetabulum following TPO, has been associated with the use of dynamic compression plates (DCP) and with the angle of the iliac osteotomy[39]. The subsequent lateralization of the hip joint increases the lever arm of the gravitational force, thus the magnitude of the abductor and hip reaction forces. This, in turn, offsets the beneficial effect of medialization of the femoral head following its relocation. In this study, pre-angled TPO plates were used (instead of DCPs) to stabilize the ilium.

Furthermore, osteotomy of the ilium was performed perpendicularly to the long axis of the pelvis rather than ilium. As a consequence, lateralization of the acetabular fragment was not observed. Indeed, the position of the geometrical center of the acetabulum with respect to the sagittal plane was not affected by the TPO procedure. This agrees with the findings of a previous *in vitro* study which examined the alteration in pelvic anatomy after TPO[39].

Following TPO, the direction of the abductor muscle force (given by the angle θ_a) was altered towards the vertical as ventroversion of the acetabulum increased. This was explained by the reduction of the projected distance between the points of origin and insertion of the abductor muscles as the femur moved closer to the sagittal plane. Consequently, the orientation of the hip reaction force, (given by the angle θ_h) followed the same trend. An effect of the increase of θ_h is the decrease of the horizontal component of F_h. This may be the consequence of a reduction of the force needed to counteract the subluxation of the hip as the containment of the joint improves.

The forces acting on the canine hip in both dynamic and static conditions are complex. The orientation and magnitude of muscle forces in the actual 3-dimensional geometry of the hip joint form a system that is very difficult to model. Indeed, variations in the muscle mass and conformation of animals coupled with the lack of information on the relative strength of contraction of various muscles surrounding the hip would require that many unsubstantiated assumptions be used in creating such a model. The 2-

dimensional mathematical model used in this study was adapted from the classic description of Pauwels' static mechanical model[105]. While this model does have certain limitations (lack of 3-dimensional anatomic orientation of muscles, absence of controlled muscle forces) we feel it does provide a unique tool with which to examine the effect of alterations of the pelvic geometry on the forces acting about the hip joint.

In man, procedures which reduce hip loads alone (i.e., weight loss, changing weight distribution through the use of a cane or by adopting an antalgic gait and varus osteotomies) do not produce long term favorable results unless stability and congruity of the joint are also improved[88, 109, 134]. In addition to reducing the hip reaction force, procedures which restore joint stability and increase the weight-bearing area upon which the force is applied could greatly contribute to the reduction of the stress imposed on the articular cartilage[119]. Although previous studies have subjectively described the increase in femoral coverage following TPO[29, 53, 139, 147], the effect of the procedure on hip containment and articular contact areas had yet to be investigated.

In this study, the center-edge angle omega (ω) measured at the level of the maximum diameter of the hip was used to evaluate the degree of femoral head coverage by the acetabulum. The angle of coverage, determined from transverse computerized tomography (CT) scan images, reflects containment of the femoral head by the acetabulum and as such is a marker of joint stability. Omega was 99° in normal, stable hips. This angle is similar to the Norberg angle used to evaluate hip dysplasia from ventrodorsal radiographs. However, the lateral prominence of the cranial acetabulum (insertion of the rectus femoris) apparent on ventrodorsal OFA radiographs accounts for the relatively larger value of the Norberg angle in normal dogs (115°). The most significant improvement in coverage was observed between 0° and 20° of AVV (respectively 62° +/- 8.7° and 104° +/- 1.9°) and corresponded to reduction of the initial subluxation. Beyond 20° of AVV, coverage expectedly increased by 10° increments thus reflecting the increase in plate angle. Interestingly, the angle of coverage of dysplastic hips after reduction of the initial subluxation (20° of AVV) was slightly, however significantly, larger than that of non-dysplastic hips (104° and 99° respectively). This increase in femoral head containment by the acetabulum presumably accounts for the intrinsic stability of the dysplastic hips at 20° of AVV.

Unlike containment which relates to the configuration of the hip, congruity refers to contact between opposing articular surfaces. As such, congruity is a better measure of articular stresses. Indeed, a dysplastic hip can be stable because it is well contained after large acetabular correction (such as in Chiari's procedure) but poorly congruent because of alteration of the geometry of the femoral head or the acetabulum, or both. Loss of congruence, i.e. loss of contact, translates into alteration of stress distribution and magnitude and eventually leads to degeneration of the articular cartilage[87, 119]. Although coverage increases with TPO[29, 53], the effect of the procedure on joint contact remained unknown. In this study, articular contact was evaluated using computerized tomography. Contact between opposing articular surfaces was accentuated by using intra-articular contrast medium. Unlike dye staining, cast or pressure sensitive film techniques, this protocol preserves the integrity of the joint capsule, thus allowing loading of the hip in subluxated positions. Furthermore, the configuration of the joint was not altered by the presence of viscous (rubber cast) or stiff (pressure sensitive film) material interposed between articular surfaces. In addition, by integrating elementary surfaces in the cranio-caudal direction, this technique reflects the 3 dimensional shape of the actual surface of contact. However, because of the tangential orientation of the CT images, this method does not permit precise measurement of the surfaces of the cranial and caudal poles of the joint. As a consequence, the computed surfaces probably underestimated the actual magnitude of the contact area between femoral head and acetabulum. Nevertheless, as this study investigated the relative changes in contact area after TPO rather than their actual magnitude, it is unlikely that the results were affected by the method. Stereo-photogrammetry techniques have been shown to provide a more accurate estimate of articular contact areas, however, the method is not readily available[4].

In this study, reduction of the initial subluxation at 20° of acetabular ventroversion resulted in a highly significant increase in articular contact area. A slight, although significant, increase persisted between 20° and 30° of acetabular ventroversion. As AVV increased beyond 30°, the surface of contact remained virtually unchanged. A probable explanation for this pattern of change in articular contact can be inferred when considering the spherical covering of the femoral head by the acetabulum. Indeed, once reduction has occurred, an increase in AVV merely results in a reorientation of the horse shoe shaped acetabulum without substantially affecting the magnitude of the contact area. A direct and undesirable effect of the increase in AVV and coverage is the lateral shift of the acetabular rim closer to the femoral neck. This, in turn, may contribute to the reported reduction in hip range of motion especially in abduction[140] and to the higher risk of medioventral luxation of the femoral head following TPO[150]. In this study, despite the similarity in magnitude, the percentage of articular contact of normal hips was significantly smaller than that of dysplastic hips after reduction. (17.4% versus 20.1% respectively). In normal hips, the acetabular roof is horizontal[43] and, as shown by the relatively small angle of coverage, the lateral rim of the acetabulum only slightly extends over the geometrical center of the femoral head. These anatomic traits likely account for the inherent stability of the hip joint while providing the minimal amount of laxity essential to joint motion. An increase in AVV alters this equilibrium and tends to seat the femoral head deeper in the acetabulum, thus increasing the surface of contact especially when the joint is loaded.

Despite its spherical appearance, the unloaded hip is a relatively incongruent joint when compared to joints such as the elbow[145]. In addition, the horse shoe shape of the acetabulum substantially decreases the amount of cartilage available for articular contact in any given configuration. However, because of its open shape, the acetabulum can spread under high loads, thus increasing the surface available for articular contact[119]. Furthermore, load bearing articular surfaces, are covered by a thicker cartilage which also deforms under loads thus improving the congruity of the joint (Figure D1). Both the change in acetabular geometry and the flattening of the articular cartilage under load contribute to increasing the load bearing area thus decreasing the magnitude of articular stresses[119, 145]. In normal hips, the femoral articular cartilage is thicker near the fovea and becomes thinner towards the periphery of the femoral head while the acetabular cartilage is thicker along the labrum[35, 119]. Following TPO, changes in orientation, rather than magnitude, of the surface of contact may partially explain the continuous, although slower, progression of osteoarthrosis reported postoperatively[83, 140] despite improvement in joint stability[83]. Indeed, as AVV increases, the articular surface of the acetabulum moves away from the dorsal aspect of the femoral head. Consequently, the thicker acetabular cartilage faces the thinner articular cartilage at the periphery of the femoral head (Figure D2). As a result of this relative difference in structural properties, the acetabular cartilage may be subjected to higher strains and may become more susceptible to fatigue failure and degenerative changes[145].

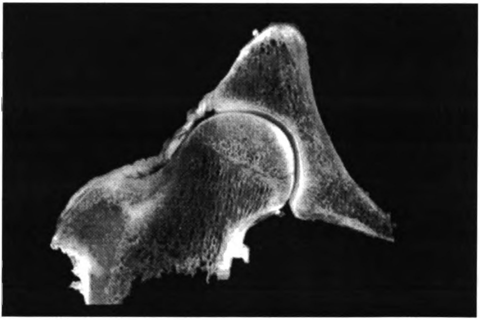

Figure D1 - Cross section of an unloaded canine hip joint in a neutral position. Congruity is achieved in part through variation in femoral and acetabular cartilage thickness.

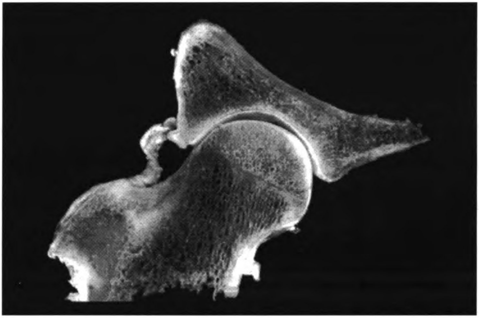

Figure D2 - Cross section of the same joint with 40° of AVV. Incongruity partially results from alteration of the normal articular cartilage relationship and absence of load.

From a mechanical standpoint, stress reduction is optimal when the hip reaction force is perpendicular to the load bearing area and passes near its geometrical center[109]. Although not directly measured in this study, the effect of TPO on the relative position of the hip reaction force in relation to the surface of contact has been subjectively estimated. At the level of the maximum diameter of the femoral head, the angle intercepting the surface of contact was approximately 40° in both normal and reduced dysplastic hips. As the angle of AVV increased, the position of the surface of contact rotated laterally while the orientation of the hip force increased towards the vertical. The rates of change were, however, substantially different. Consequently, the acetabular contact area progressively moved away from the hip force, thus becoming a "non-functional" load bearing surface (Figure D3). The significance of this finding is conjectural and may imply that the hip reaction force passes somewhat lateral to the femoral head rather than through its geometrical center as theorized in this study. At this point however, this assumption remains speculative and has not been verified. Nevertheless, it is conceivable that the alteration of the position of the contact area in relation to the hip force may have a deleterious effect on the distribution and magnitude of the stresses imposed on the articular cartilage. Based on these observations, it appears that the risk of osteoarthrosis increases with the degree of AVV. This analysis agrees with clinical findings[83, 150].

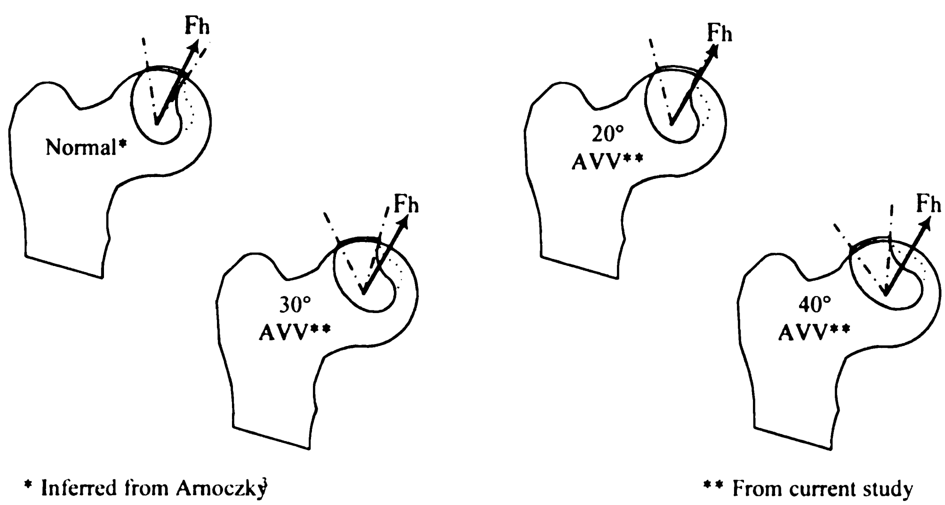

Figure D3 - Diagram illustrating the effect of AVV on the relative position of the hip force (F_h) in relation to the surface of articular contact (shaded area).

The results of previous studies have shown that the main adverse effects of TPO result from a substantial decrease in the range of motion of the hip, mainly in abduction but also in flexion and extension[140, 147, 148], and from a severe reduction of the pelvic inlet[39].

While precise guidelines for plate selection have not been established, in most clinical situations, the choice of a plate is based on the Ortolani sign[101]. The "angle of reduction" and the "angle of subluxation" of the hip respectively represent the maximal and minimal angles of acetabular rotation needed to provide joint stability[147]. Because excessive AVV may be associated with femoral neck impingement on the acetabular rim and tendency for medial luxation of the hip, selection of the minimal angle necessary to maintain joint stability has been recommended[148]. The magnitude of this angle, however, had yet to be determined. In this study, using a custom designed "hinge plate", it was shown that spontaneous relocation of the femoral head occurred on average at approximately 17.2° of acetabular ventroversion. This angle represents the minimal angle of AVV necessary to attain stable reduction of the hip joint. Since changes in the angle of AVV parallel changes in the angle of coverage, this minimal angle of reduction corresponds to a angle of coverage of approximately 101°, very similar to that of normal dogs (99°). The results of this study also revealed that the Ortolani angle of reduction was significantly larger than its experimental counterpart. Moreover, there was no significant correlation between the two methods. Several reasons may explain these discrepancies. Due to the pelvic and femoral musculature, the actual positions of the femur and hip are subjectively estimated. Consequently, interpretation of the Ortolani angle of reduction may vary substantially from dog to dog depending on the animal's anatomy. In addition, the manual load placed upon the femur while abducting the leg tends to rotate the femur beyond the point of actual hip relocation therefore overestimating the angle of reduction. Finally, due to the caudomedial tilt of the ilium, the experimental angle of reduction is underestimated by approximately 3.5°, which also contributes to the discrepancy between the two methods.

The results of this study suggest that TPO decreases the magnitude of the forces acting about the coxofemoral joint by inducing reduction and subsequent medialization of the subluxated femoral head. In addition, the TPO procedure increases the area of articular contact between femoral head and acetabulum. Both factors likely contribute to the beneficial clinical results reported following TPO by lowering the magnitude of the stress imposed on the articular cartilage. Likewise, the increase in coverage improves the stability of the joint, thus the biomechanical efficiency of the abductor muscles and, as suggested by Pauwels[109], results in a more even distribution of the articular stress over the load bearing area. This study also demonstrated that both the configuration and biomechanics of dysplastic joints after reduction was similar to that of normal hips. Based on these observations, it is conceivable that increasing the AVV angle beyond 20° may not significantly improve the beneficial effects of TPO and, therefore, should be carefully weighed against the increased risk of postoperative complications associated with large angles of correction.

It is important to keep in mind that this study is an *in vitro* study. As such, it should be considered only as a first step towards a better understanding of the effect of TPO on the biomechanics of the hip joint. Although we believe that the information provided may help orthopaedic surgeons in choosing the most appropriate angle of acetabular ventroversion, we also realize that results may vary in clinical situations. In order to validate the results of this study, long term prospective clinical trials evaluating the effects of the age at which TPO is performed and magnitude of AVV should be implemented. In the mean time, cautious interpretation of these results is recommended.

CONCLUSIONS

1. Subluxation of the hip joint secondary to canine hip dysplasia results in an increase in the magnitude of the forces acting about the hip joint, a decrease in the surface of contact between femoral head and acetabulum and a decrease in the coverage of the femoral head by the acetabulum.

2. Triple pelvic osteotomy used as a treatment of hip dysplasia decreases the magnitude of the hip forces and increases both articular contact and acetabular coverage. It also improves the stability of the joint. These changes result from medialization of the femoral head following stable reduction of the initial hip subluxation.

3. With triple pelvic osteotomy, stable reduction of coxofemoral subluxation occurs for acetabular ventroversion angles smaller than 20° (on average, approximately 17.2°).

4. Following TPO, the biomechanics and configuration of dysplastic hips, once reduction of the initial subluxation has occurred, are similar to those of normal hips.

5. When using triple pelvic osteotomy, no significant changes in hip biomechanics and configuration occur beyond 30° of acetabular ventroversion.

6. The Ortolani angle of reduction tends to overestimate the magnitude of the acetabular ventroversion needed to achieve joint stability.

APPENDICES

APPENDIX A

APPENDIX A

Clinical recording of the Ortolani angles of reduction and luxation.

The Ortolani sign was evaluated while the dogs were under anesthesia. Each animal was placed on dorsal recumbency with its knee flexed and the femurs held vertically. Coxofemoral subluxation was obtained by applying firm pressure to the hip through the femur. While maintaining axial compression, the femur was slowly abducted until a distinct "click" corresponding to the relocation of the femoral head into the acetabulum occurred (Figure A1). This click is referred to as the Ortolani sign. A goniometer was used to record this angle of reduction. The leg was then slowly returned to a vertical position and the angle at which subluxation occurred was similarly recorded. This angle is called the angle of subluxation. Subluxation is accompanied with a distinct sound referred to as the Barlow sign.

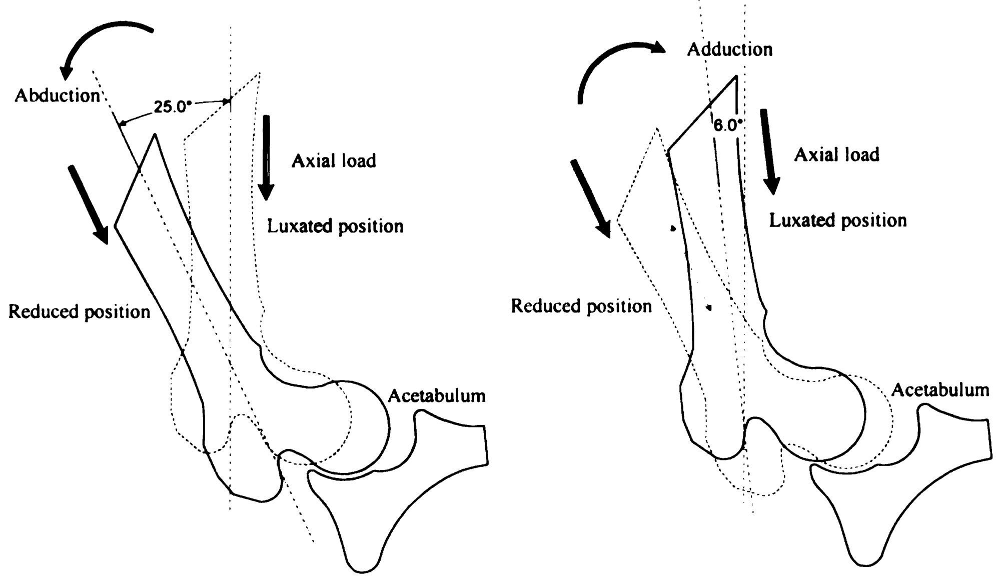

Figure A1 Line drawing illustrating the measurement of the Ortolani angles of reduction (left) and subluxation (right). In most clinical situations, the choice of a TPO plate is based on the Ortolani sign. The angle of reduction and the angle of subluxation of the hip respectively represent the maximal and minimal angles needed for acetabular rotation to provide stability. In this example, a 20° TPO plate would be recommended.

APPENDIX B

APPENDIX B

Strain gage selection and calibration protocol.

Strain gages and technical support: Tech Notes (TN) and Tech Tips (TT) provided by:
Measurements Group, Inc.
P.O. Box 27777
Raleigh, NC 27611
Phone: (919) 365 3800
Fax: (919) 365 3945

Gage selection (TN-505-3)

Accurate measurement of strain requires selection of the appropriate gage for the task. Parameters such as nature of the backing material (carrier), loading condition (cyclic, axial, bending), temperature, and anticipated elongation, may affect the operating characteristics of a strain gage and are important to consider in the selection of a gage.

In this experiment, a nylon rod ("nylon general purpose", Laird Plastics, Grand Rapids, Michigan) was axially loaded at room temperature. The potential strain ε of the rod was determined from its material properties (elastic modulus E = 400,000 psi) its structural properties (cross section $A = 0.11\ in^2$) and the range of desired load P (35 lbs to 50 lbs) using the following equation: $\varepsilon = P/AE$. Thus, $0.09\% < \varepsilon < 0.13\%$.

Based on the value of the expected strain, a "EA general purpose" strain gage was recommended (gage type EA-13-120LZ-120). These gages are appropriate for use on metal or plastic (nylon) carriers, are self-temperature-compensated and can see a strain of up to 3%. Application of the gages was performed according to the technical tips TT-603, 604, 606, 609 and B-127-13 from Measurements Group, Inc.

Gage calibration

As strain gages are extremely sensitive to stretching, an unevenly loaded rod would yield aberrant and unrepeatable readings from the strain gage indicator. This problem was eliminated by placing 2 strain gages opposite to one another and by designing a loading bar which could act as a universal joint, thus allowing for uniaxial loading. Although the strain gages used in this study were self-temperature-compensated, two additional gages were mounted on a "dummy" nylon rod to completely eliminate the effect of temperature. The final device thus featured 2 "active" gages for strain measurement and 2 "passive" gages for temperature compensation.

The 4 strain gages were connected to a Strain Indicator P-3500 (Measurements Group) in a full bridge design, then, the gage factor (2.095 ± 0.5%), specific to the gage in use, was entered into the Strain Indicator.

The "active" rod was then calibrated using dead weights in 5 pound increment (from 0 to 50 lbs) while the "dummy" rod remained passive. Creeping of the nylon rod was taken into consideration by waiting for a period of 15 minutes under maximum load (55 lbs), then 5 minutes between each 5 pound increment from 0 to 50 lbs.

The strain indicator displayed a linear strain / load relationship with a regression coefficient $r^2 = 0.99$. The results were consistent from trial to trial during calibration. The following data was representative of the calibration procedure.

Load X (lbs)	0	5	10	15	20	25	30	35	40	45	50
Output Y ($\mu\varepsilon$)	5	53	102	152	202	255	306	357	408	466	518

Output Y = f (Load X) is a linear relationship such as $Y \cong 10X + 5$ which meant that each pound of load approximately corresponded to 10 $\mu\varepsilon$.

APPENDIX C

APPENDIX C

Radiographic evaluation of the actual angle of acetabular ventroversion

The actual value of the AVV angle evaluated radiographically. Three metallic pins were aligned on the dorsal aspect of the ilium so that only one pin could be seen on a cranio-caudal radiograph. Two pins were implanted cranial to the planed osteotomy site and served to verified proper alignment and positioning of the pelvis. The third pin placed caudal to the osteotomy site indicated the acetabulum ventroversion angle. The anatomic tilt of the ilium was determined before osteotomy using the hinge-plate, its value was -6° in this experiment. Then the osteotomy was performed and the 20° pre-angled TPO plate applied. A cranio-caudal radiograph was then obtained, from which the actual angle of ventroversion was measured. The procedure was repeated with the 30° and 40° plates. As expected the actual angle of acetabular ventroversion were successively 26°, 36° and 46°.

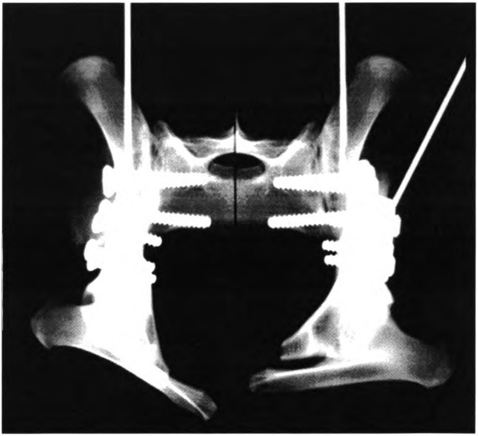

Figure A2 - Radiographs demonstrating the actual value of the AVV angle when using a TPO plate. A 20° TPO plate produced a 26° ventroversion of the acetabulum (right).

APPENDIX D

APPENDIX D

Data sheets for the anatomical and clinical studies

Dog # 1 | BW # 66 | F < 18 months | Yellow Lab.

PHYSICAL | Ortolani | Left | | Right*
Reduction 27° | Reduction 25°
Luxation 3° | Luxation 0°

PHYSICAL	Ortolani	Left		Right*	
		Reduction	27°	Reduction	25°
		Luxation	3°	Luxation	0°
RADIOLOGY	No DJD				
	Neck angle	Left	135°	Right*	132°

CT SCAN *(Left side read corresponds to actual Right side)

Head ∅ (Dm)	Right 23 mm				Angle of coverage (ω) @ Dm (right)			
Head area (Cm)	Right 831 mm2							
AVV	0°	20°	30°	40°	0°	20°	30°	40°
Contact area (C)	40.25	164.52	173.08	177.11				
C% = C/Cm	4.8	19.8	20.8	21.3	70°	103°	116°	125°

REDUCTION STUDY	Left	Red.	18°	Right Red.	17°
		Lux.	6°	Lux.	7°
		Cor.	-4°	Cor.	-4°

Arc / Surface measurement

$A = (2.\pi / 360) . R\alpha = \pi/360 . D\alpha = A$

with A: arc of circle
R: radius & D: diameter of head on given slice
α: angle intercepting A

$dS = A.dx = \pi/360 \ 1.5 \ D\alpha$

with dS: elementary surface of a scan slice
dx: thickness of a scan slice i.e. 1.5 mm

$C = \Sigma dS$

with C: absolute contact area

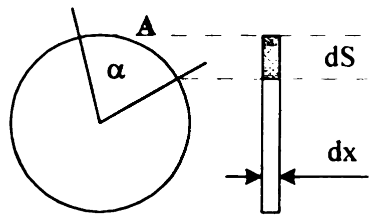

$dS = 0.01309 \ (D.\alpha)$

Coverage measurement

ω = angle of coverage @ the level of Dm

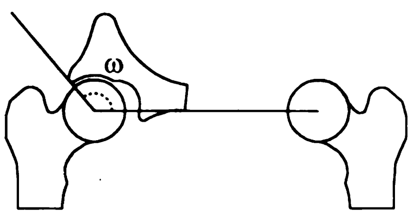

Approximations

1) head is spherical and total head surface is $Hs = \pi.D_m^2$

2) Maximum contact surface Cm is less than 1/2 that of a sphere having for diameter the maximum diameter D_m of the head measured on the scan, thus $Cm = \pi.D_m^2 / 2$

with $D_m = 23$ mm $Cm = 831$ mm2

3) contact area can be expressed as a % of the surface of the head: $C\% = C / Cm$

Dog # 2 BW # 63 F < 18 months Yellow Lab.

<u>PHYSICAL</u>	Ortolani	Left*		Right	
		Reduction	25°	Reduction	30°
		Luxation	8°	Luxation	7°
<u>RADIOLOGY</u>	No DJD				
	Neck angle	Left*	135°	Right	136°

<u>CT SCAN</u> *(Right side read corresponds to actual Left side)

Head Ø (Dm)	Left 23 mm				Angle of coverage (ω) @ Dm (left)			
Head area (Cm)	Left 831 mm2							
AVV	0°	20°	30°	40°	0°	20°	30°	40°
Contact area (C)	24.58	173.28	180.12	178.46				
C% = C/Cm	2.9	20.8	21.7	21.5	61°	103 °	112 °	122 °

<u>REDUCTION STUDY</u>	Left	Red.	17°	Right	Red.	19°
		Lux.	6°		Lux.	7°
		Cor.	-4°		Cor.	-4°

<u>Arc / Surface measurement</u>

$A = (2.\pi / 360) . R\alpha = \pi/360 . D\alpha = A$

with A: arc of circle

R: radius & D: diameter of head on given slice

α: angle intercepting A

$dS = A.dx = \pi/360\ \ 1.5\ \ D\alpha$

with dS: elementary surface of a scan slice

dx: thickness of a scan slice i.e. 1.5 mm

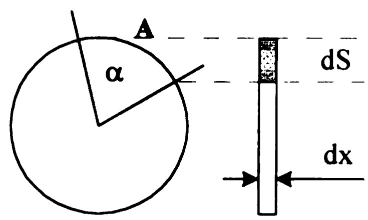

$dS = 0.01309\ (D.\alpha)$

$C = \Sigma dS$

with C: absolute contact area

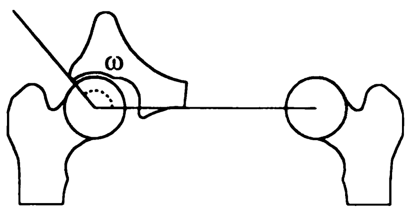

<u>Coverage measurement</u>

ω = angle of coverage @ the level of Dm

<u>Approximations</u>

1) head is spherical and total head surface is $Hs = \pi.D_{m.}^{2}$

2) Maximum contact surface Cm is less than 1/2 that of a sphere having for diameter the maximum diameter D_m of the head measured on the scan, thus $Cm = \pi.D_{m.}^{2} / 2$

with $D_m = 23$ mm Cm = 831 mm2

3) contact area can be expressed as a % of the surface of the head: C% = C / Cm

Dog # 3 BW # 61 M < 18 months Black Lab.

PHYSICAL Ortolani

	Left		Right*	
	Reduction	31°	Reduction	29°
	Luxation	8°	Luxation	6°

RADIOLOGY No DJD

Neck angle Left 138° Right* 137°

CT SCAN *(Left side read corresponds to actual Right side)

Head ∅ (Dm)	Right 23 mm				Angle of coverage (ω)			
Head area (Cm)	Right 831 mm2				@ Dm (right)			
AVV	0°	20°	30°	40°	0°	20°	30°	40°
Contact area (C)	43.66	162.96	177.43	184.2				
C% = C/Cm	5.2	19.6	21.3	22.2	72°	107°	120°	130°

REDUCTION STUDY

	Left		Right	
	Red.	18°	Red.	15°
	Lux.	0°	Lux.	0°
	Cor.	-4°	Cor.	-4°

Arc / Surface measurement

$A = (2.\pi / 360) . R\alpha = \pi/360 . D\alpha = A$

with A: arc of circle

R: radius & D: diameter of head on given slice

α: angle intercepting A

$dS = A.dx = \pi/360 \ 1.5 \ D\alpha$

with dS: elementary surface of a scan slice

dx: thickness of a scan slice i.e. 1.5 mm

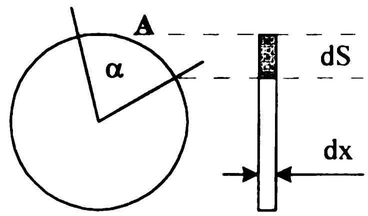

$dS = 0.01309 (D.\alpha)$

$C = \Sigma dS$

with C: absolute contact area

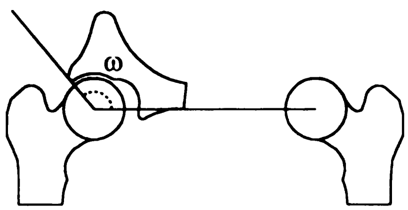

Coverage measurement

ω = angle of coverage @ the level of Dm

Approximations

1) head is spherical and total head surface is $Hs = \pi.D_m^2$

2) Maximum contact surface Cm is less than 1/2 that of a sphere having for diameter the maximum diameter D_m of the head measured on the scan, thus $Cm = \pi.D_m^2 / 2$

with $D_m = 23$ mm $Cm = 831$ mm2

3) contact area can be expressed as a % of the surface of the head: $C\% = C / Cm$

Dog # 4 BW # 62 F < 18 months Black Lab.

PHYSICAL Ortolani Left* Right
Reduction 28° Reduction 30°
Luxation 5° Luxation 5°

RADIOLOGY No DJD
Neck angle Left* 131° Right 132°

CT SCAN *(Right side read corresponds to actual Left side)

Head ∅ (Dm)	Left 21 mm				Angle of coverage (ω)			
Head area (Cm)	Left 693 mm2				@ Dm (left)			
AVV	0°	20°	30°	40°	0°	20°	30°	40°
Contact area (C)	30.21	131.06	140.8	141.37				
C% = C/Cm	4.3	18.9	20.3	20.4	54°	103°	112°	121°

REDUCTION STUDY Left Red. 19° Right Red. 16°
Lux. 6° Lux. 3°
Cor. -3° Cor. -3°

Arc / Surface measurement
$A = (2.\pi / 360) . R\alpha = \pi/360 . D\alpha = A$
with A: arc of circle
R: radius & D: diameter of head on given slice
α: angle intercepting A
$dS = A.dx = \pi/360\ 1.5\ D\alpha$
with dS: elementary surface of a scan slice
dx: thickness of a scan slice i.e. 1.5 mm
$C = \Sigma dS$
with C: absolute contact area

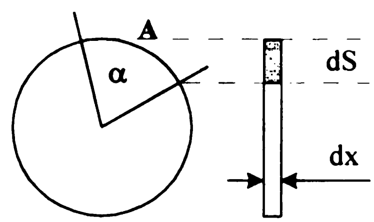

$dS = 0.01309\ (D.\alpha)$

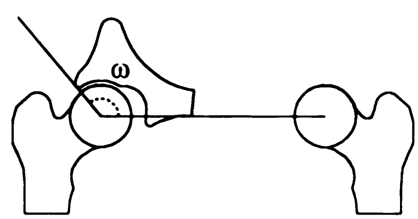

Coverage measurement
ω = angle of coverage @ the level of Dm

Approximations
1) head is spherical and total head surface is $Hs = \pi.D_m^2$
2) Maximum contact surface Cm is less than 1/2 that of a sphere having for diameter the maximum diameter D_m of the head measured on the scan, thus $Cm = \pi.D_m^2 / 2$
with $D_m = 21$ mm $Cm = 693$ mm2
3) contact area can be expressed as a % of the surface of the head: $C\% = C / Cm$

Dog # 5 BW # 67 M < 18 months Black Lab.

PHYSICAL Ortolani

	Left		Right*	
	Reduction	32°	Reduction	31°
	Luxation	8°	Luxation	5°

RADIOLOGY No DJD

	Left		Right*	
Neck angle	Left	137°	Right*	136°

CT SCAN *(Left side read corresponds to actual Right side)

Head ∅ (Dm)	Right 23 mm				Angle of coverage (ω)			
Head area (Cm)	Right 831 mm2				@ Dm (right)			
AVV	0°	20°	30°	40°	0°	20°	30°	40°
Contact area (C)	44.12	172.42	179.73	171.27				
C% = C/Cm	5.3	20.7	21.6	20.6	65°	107°	122°	134°

REDUCTION STUDY

		Left			Right
Red.	15°		Red.	17°	
Lux.	0°		Lux.	1°	
Cor.	-4°		Cor.	-3°	

Arc / Surface measurement

$A = (2.\pi / 360) . R\alpha = \pi/360 . D\alpha = A$

with A: arc of circle
R: radius & D: diameter of head on given slice
α: angle intercepting A

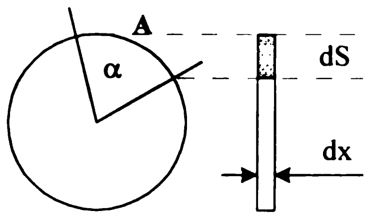

$dS = A.dx = \pi/360\ \ 1.5\ \ D\alpha$

with dS: elementary surface of a scan slice
dx: thickness of a scan slice i.e. 1.5 mm

$dS = 0.01309\ (D.\alpha)$

$C = \Sigma dS$

with C: absolute contact area

Coverage measurement

ω = angle of coverage @ the level of Dm

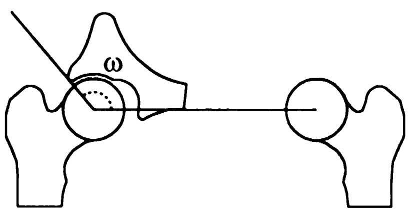

Approximations

1) head is spherical and total head surface is $Hs = \pi.D_m^{\ 2}$

2) Maximum contact surface Cm is less than 1/2 that of a sphere having for diameter the maximum diameter D_m of the head measured on the scan, thus $Cm = \pi.D_m^{\ 2} / 2$

with $D_m = 23$ mm $Cm = 831$ mm2

3) contact area can be expressed as a % of the surface of the head: $C\% = C / Cm$

Dog # 6 | BW # 68 | M < 18 months | Yellow Lab.

PHYSICAL — Ortolani — Left: Reduction 30°, Luxation 0° — Right*: Reduction 35°, Luxation 5°

RADIOLOGY — No DJD — Neck angle: Left 136°, Right* 134°

CT SCAN *(Left side read corresponds to actual Right side)

Head ∅ (Dm)	Right 24 mm				Angle of coverage (ω) @ Dm (right)			
Head area (Cm)	Right 905 mm2							
AVV	0°	20°	30°	40°	0°	20°	30°	40°
Contact area (C)	30.05	189.14	189.87	190.44				
C% = C/Cm	3.3	20.9	21	21	50°	105 °	113 °	123 °

REDUCTION STUDY — Left: Red. 17°, Lux. 3°, Cor. -3° — Right: Red. 18°, Lux. 6°, Cor. -3°

Arc / Surface measurement

$A = (2.\pi / 360) . R\alpha = \pi/360 . D\alpha = A$

with A: arc of circle

R: radius & D: diameter of head on given slice

α: angle intercepting A

$dS = A.dx = \pi/360 \ 1.5 \ D\alpha$

with dS: elementary surface of a scan slice

dx: thickness of a scan slice i.e. 1.5 mm

$C = \Sigma dS$

with C: absolute contact area

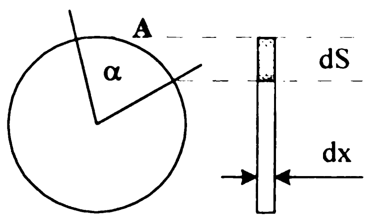

$dS = 0.01309 (D.\alpha)$

Coverage measurement

ω = angle of coverage @ the level of Dm

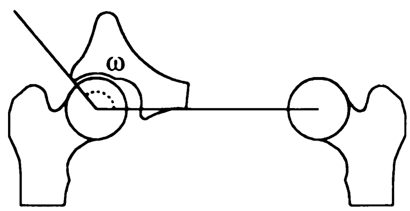

Approximations

1) head is spherical and total head surface is $Hs = \pi.D_m^2$

2) Maximum contact surface Cm is less than 1/2 that of a sphere having for diameter the maximum diameter D_m of the head measured on the scan, thus $Cm = \pi.D_m^2 / 2$

with $D_m = 24$ mm $Cm = 905$ mm2

3) contact area can be expressed as a % of the surface of the head: $C\% = C / Cm$

Normal # 1 BW # 30 M < 3 years Mix Breed

PHYSICAL Ortolani Left None Right None

CT SCAN (Left scan read corresponds to actual right side)

Head ∅ = Dm	Right 16 mm	Angle of coverage @ Dm
Head area Cm	Right 402 mm2	**98°**
Contact area C	70.13	
C% = C / Cm	**17.4**	

Normal # 2 BW # 70 M < 3 years Mix Breed

PHYSICAL Ortolani Left None Right None

CT SCAN (Right scan read corresponds to actual left side)

Head ∅ = Dm	Left 25 mm	Angle of coverage @ Dm
Head area Cm	Left 982 mm2	**98°**
Contact area C	172.16	
C% = C / Cm	**17.5**	

Normal # 3 BW # 55 M < 3 years Eng. Pointer

PHYSICAL Ortolani Left None Right None

CT SCAN (L scan read corresponds to actual R side)

Head ∅ = Dm	Right 23 mm	Angle of coverage @ Dm
Head area Cm	Right 831 mm2	**100°**
Contact area C	143.71	
C% = C / Cm	**17.3**	

Normal # 4 BW 42 # M < 3 years Mix Breed

PHYSICAL Ortolani Left None Right None

CT SCAN (Left scan read corresponds to actual right side)

Head ∅ = Dm	Right 21 mm	Angle of coverage @ Dm
Head area Cm	Right 693 mm2	**101°**
Contact area C	122.45	
C% = C / Cm	**17.7**	

Normal 5 BW 50 # M < 3 years Mix Breed

PHYSICAL Ortolani Left None Right None

CT SCAN (Right scan read corresponds to actual left side)

Head ∅ = Dm	Left 22 mm	Angle of coverage @ Dm
Head area Cm	Left 760 mm2	**99°**
Contact area C	130.65	
C% = C / Cm	**17.2**	

LIST OF REFERENCES

LIST OF REFERENCES

1. Afoke NYP et al: The incongruous hip joint. J Bone Joint Surg, [Br], 62(4):511-514, 1980

2. Alexander JW: The pathogenesis of canine hip dysplasia. Vet Clin North Am Small Anim Pract, 22(3):503-511, 1992

3. Arnoczky SP, Torzilli PA: Biomechanical analysis of the forces acting about the canine hip. Am J Vet Res, 42:1581-1585, 1981

4. Ateshian GA et al: A stereophotogrammetric method for determining in situ contact areas in diarthrodial joints and a comparison with other methods. J Biomech, 27(1):111-124, 1994

5. Athanasiou KA et al.: Biomechanical properties of the hip cartilage in experimental animal models. Clin Ortho, 316:254-266, 1995

6. Badoux DM: General biostatics and biomechanics. In: R Guetty, ed. Sisson and Grossman's Anatomy of the domestic animals, 5th ed., Vol. 1. Philadelphia, WB Saunders, pp. 48-83, 1975

7. Bardens JW, Hardwick H: New observation on the diagnosis and cause of hip dysplasia. Vet Med Small Anim Clin, 63:238-245, 1968

8. Barlow TG: Early diagnosis and treatment of congenital dislocation of the hip. J Bone Joint Surg [Br], 44:292-306, 1962

9. Barr AR et al: Clinical hip dysplasia in growing dogs: the long term result of conservative management. J Small Anim Pract, 28:243-252, 1987

10. Belkoff SM, Padgett G, Soutas-Little RW: Development of a device to measure canine coxofemoral joint laxity. Vet Comp Orthop Trauma, 1:312-36, 1989

11. Belfield WO: Chronic subclinical scurvy and canine hip dysplasia. Vet Med Small Anim Clin, 74:1399-1401, 1976

12. Bennett D: Hip dysplasia and ascorbate therapy: fact or fancy? Sem Vet Med Surg, 2(2):152-157, 1987

13. Berzon JL et al: A retrospective study of the efficacy of the femoral head and neck excisions in 94 dogs and cats. Vet Surg, 9:88-92, 1980

14. Bombelli R et al: Mechanics of the normal and orteoarthritic hip. Clin Orthop, 182:69-78, 1984

15. Braden TD, Prieur DW: Three plane intertrochanteric osteotomy for the treatment of early stage hip dysplasia. Vet Clin North Am Small Anim Pract, 22(3):623-643, 1992

16. Brass W: Hip dysplasia in dogs. J Small Anim Pract, 30:166-170, 1989

17. Brinker WO: Corrective osteotomy procedures for treatment of canine hip dysplasia. Vet Clin North Am Small Anim Pract, 1(3):467-477, 1971

18. Brinker WO, Flo GL, Cross JF: Acetabuloplasty as a corrective surgical procedure in selected cases of congenital hip dysplasia in the dog. Proc Annu Meet Am Anim Hosp Assoc, pp. 260-262, 1968

19. Brown TD, Shaw DT: In vitro contact stress distribution on the femoral condyles. J Orthop Res, 2:190-199, 1984

20. Budesberg S, Verstraete M, Soutas-Little RW: Force plate analysis of the walking gait in healthy dogs. Am J Vet Res 48:915-918, 1987

21. Chalman JA, Butler HC: Coxofemoral laxity and the Ortolani sign. J Am Anim Hosp Assoc, 21:671-676, 1985

22. Chapchal GJ: The intertrochanteric osteotomy in the treatment of congenital dysplasia of the hip. Clin Orthop, 119:54-59, 1976

23. Chapchal GJ: Indications of the various types of pelvic osteotomy. Clin Orthop, 98:111-115, 1974

24. Chiari K: Ergebnisse mit der beckenosteotomie als pfannendachplastik. Z. Orthop, 87:14, 1955

25. Chiari K: Medial displacement osteotomy of the pelvis. Clin Orthop 98:55-71, 1974

26. Chung SM: Biomechanics of the developing hip joint. In: Hip disorders in infants and children. Philadelphia, Lea & Febiger, 1981

27. Corley EA: Hip dysplasia: a report from the Orthopaedic Foundation for Animals. Sem Vet Med Surg, 2(2):141-151, 1987

28. Corley EA, Keller GG: Hip dysplasia: A progress report and update. Orthopaedic Foundation for Animal, Columbia, MO, pp. 1-20, 1993

29. Datt SC, Rudy RL: Development of a technique for acetabular rotation as a possible treatment of chronic coxofemoral subluxation in the dog. Master's thesis, Ohio State University, 1966

30. DeHaan JJ et al: Evaluation of polysulfated glycosaminoglycan for the treatment of hip dysplasia in dogs. Vet Surg, 23:177-181, 1994

31. Denham RA: Hip mechanics. J Bone Joint Surg, [Br], 41:550-557, 1959

32. Devine T, Slocum B: Results of femoral neck lengthening procedure in 75 dogs (abstract). Proc Annu Meet Vet Orthop Res Soc, p 3, 1995

33. DeYoung DJ et al: Implantation of an uncemented total hip prosthesis and initial results of 100 arthroplasties. Vet Surg, 21(3):168-177, 1992

34. Douglas SW, Williamson HD: Veterinary radiological interpretation Philadelphia, Lea & Febiger, p 109, 1970

35. Evans HE, deLahunta A: The skeletal and muscular systems. In: Miller's guide to the dissection of the dog. 2nd Ed. Philadelphia, WB Saunders, 1980

36. Fry TR, Clark DM: Canine hip dysplasia: Clinical signs and physical diagnosis. Vet Clin North Am Small Anim Pract, 22(3)551-558, 1992

37. Ganz R et al: A new periarticular osteotomy for the treatment of hip dysplasia. Technique and preliminary results. Clin Orthop, 232:26-36, 1988

38. Goodfellow JW et al: Patello-femoral joint mechanics and pathology. J Bone Joint Surg, [BR], 58(8):287-290, 1976

39. Graehler RA et al: The effects of plate type, angle of ilial osteotomy, and degree of axial rotation on the anatomy of the pelvis. Vet Surg, 23:13-20, 1994

40. Greenwald AS, O'Connor JJ: The transmission of load through the human hip joint. J Biomech, 4(6):507-528, 1971

41. Greenwald AS: Weight-bearing areas in the human hip joint. J Bone Joint Surg, [Br], 54(1)157-163, 1972

42. Greshake RJ, Ackerman N: Ultrasound evaluation of the coxofemoral joints in the canine neonate. Vet Radiol Ultrasound, 34:99-104, 1993

43. Hauptman J et al: The angle of inclination of the canine femoral head and neck. Vet Surg, 8(3):74-77, 1979

44. Hauptman J et al: Angles of inclination and anteversion in hip dysplasia. Am J Vet Res, 46(10):2033-36, 1985

45. Haut RC: Contact pressures in the patellofemoral joint during impact loading of the human flexed knee. J Orthop Res, 7:272-280, 1989

46. Hazewinkel HA: Skeletal diseases. In: Willis JM, Simpson KW, eds. The Waltham book of clinical nutrition of the dog and cat. Frome, England: Butler and Tanner, pp. 395-423, 1994

47. Hedhammer A et al: Canine hip dysplasia: Study of heritability in 401 litters of German Shepherd dogs. J AM Vet Med Assoc, 174(9):1012-1016, 1979

48. Hefti F: Spherical assessment of the hip on standard AP radiographs: A simple method for the measurement of the contact area between acetabulum and femoral head and acetabular orientation. J Pediatr Orthop, 15(6):797-805, 1995

49. Heimkes B et al: Forces acting on the juvenile hip joint in the one-leg stance. J Pediatr Orthop, 13(4):431-436, 1993

50. Henricson B et al: On the etiology and pathogenesis of hip dysplasia: a comparative review. J Small Anim Pract, 7:673-688, 1966

51. Henry JD: A modified technique for pectineal tendonectomy in the dog. J Am Vet Med Assoc, 163:465-468, 1973

52. Heyman SJ et al: Biomechanical study of the effect of coxofemoral positioning on the passive hip joint laxity in dogs. Am J Vet Res, 54(2):210-215, 1993

53. Hohn RB, Janes JM: Pelvic osteotomy in the treatment of canine hip dysplasia. Clin Orthop, 62:70-78, 1969

54. Holtzinger RH et al: The therapeutic effect of carpofen (Rimadyl-V) in 209 clinical cases of canine degenerative joint disease. Vet Comp Orthop Trauma, 5:140-144, 1992

55. Hosgood G, Lewis DD: Retrospective evaluation of fixation complications of 49 pelvic osteotomies in 36 dogs. J Small Anim Pract, 34:123-130, 1993

56. Hunt GA, Litsky AS: Stabilization of canine pelvic osteotomies with AO/ASIF plates and screws. Vet Comp Orthop Trauma, 1:52-57, 1988

57. Inman VT: The functional aspects of the abductor muscle of the hip. J Bone Joint Surg 29:607-619, 1947

58. Jensen DJ, Sertl GO: Sertl shelf arthroplasty (BOP) procedure in the treatment of hip dysplasia. Vet Clin North Am Small Anim Pract. 22:683-701, 1992

59. Johnston SA: Conservative and medical management of hip dysplasia. Vet Clin North Am, 22(3):595-606, 1992

60. Kalamchi A: Modified Salter osteotomy. J Bone Joint Surg, [Am], 64:183-187, 1982

61. Kealy RD et al: Effects of limited food consumption on the incidence of hip dysplasia in growing dogs. J Am Vet Med Assoc, 201(6):857-863, 1992

62. Kealy RD et al: Effects of dietary electrolyte balance on the subluxation of the femoral head in growing dogs. Am J Vet Res, 54(4):555-562, 1993

63. Klaue K et al: CT evaluation of coverage and congruency of the hip prior to osteotomy. Clin Orthop, 232:15-25, 1988

64. Koch DA et al: Radiographic evaluation and comparison of plate fixation after triple pelvic osteotomy in 32 dogs with hip dysplasia. Vet Comp Orthop Trauma, 6:9-15, 1993

65. Kummer B: Is the Pauwels' theory of hip biomechanics still valid? A critical analysis based on modern methods. Ann Anat, 175:203-210, 1993

66. Kwak SD et al: Cartilage thickness and contact area determination in the canine knee joint. Proc Annu Meet Orthop Res Soc, p 351, 1993

67. Lewis DD: Femoral head and neck excision and the controversy concerning adjunctive soft tissue interposition. Compendium, 14(11):1463-1471, 1992

68. Lipowitz AJ: Degenerative joint disease. In: Slatter D, ed. Textbook of small animal surgery, 2nd ed. Philadelphia, WB Saunders, pp1921-1927, 1993

69. Lippincott CL: Improvement of excision arthroplasty of the femoral head and neck utilizing a biceps femoris muscle sling. J Am Anim Hosp Assoc, 17:668-672, 1981

70. Lippincott CL: Excision arthroplasty of the femoral head and neck utilizing a biceps femoris muscle sling,. Part two: the caudal pass. J Am Anim Hosp Assoc, 20:377-384, 1983

71. Lussier B et al: Evaluation of the biocompatible osteoconductive polymer (BOP) shelf arthroplasty in normal dogs (abstract). Vet Surg, 22:389, 1993

72. Lust G et al: Development of hip dysplasia in dogs. Am J Vet Res, 34(1):87-91, 1973

73. Lust G et al: Intra-articular volume and hip joint instability in dogs with hip dysplasia. J Bone Joint Surg , [Am] 62(4):576-582, 1980

74. Lust G et al: A relationship between degree of laxity and synovial fluid volume in coxofemoral joints of dogs predisposed for hip dysplasia. Am J Vet Res 41(11):55-60, 1980

75. Lust G, Summers BA: Early, asymptomatic stage of degenerative joint disease in canine hip joints Am J Vet Res, 42:1849-1855, 1981

76. Lust G et al: Effect of intramuscular administration of glycosaminoglycan polysulfates on signs of incipient hip dysplasia in growing pups. Am J Vet Res, 53:18336-1843, 1992

77. Lust G et al: Joint laxity and its association with hip dysplasia in Labrador retrievers. Am J Vet Res 54:1990-1999, 1993

78. Mackenzie SA, Oltenacu EA, Leighton W: Heritability estimate for temperament scores in German shepherd dogs and its genetic correlation with hip dysplasia. Behav Gen, 15:475-482, 1985

79. Massat BJ, Vasseur PB: Clinical and radiographic results of total hip arthroplasty in dogs: 96 cases (1986-1992). J Am Vet Med Assoc, 205(3):448-454, 1994

80. Maquet P: A biomechanical approach to the surgical treatment of osteoarthritis of the hip. Rev Med Liege, 24:146-169, 1969

81. Maquet PG et al: Femorotibial weight-bearing areas. J Bone Joint Surg, [Am], 57:766-771, 1975

82. McLaughlin RM, Miller CW: Evaluation of hip joint congruence and range of motion before and after triple pelvic osteotomy. Vet Comp Orthop Trauma, 4:65-69, 1991

83. McLaughlin RM et al: Force plate analysis of the triple pelvic osteotomy for the treatment of hip dysplasia. Vet Surg, 20(5):291-297, 1991

84. Meyer GH: Die architectur der spongiosa. Arch Anat Physiol. 34:615, 1867

85. Millis MB, Hall JE: Transiliac lengthening of the lower extremity. A modified innominate osteotomy for the treatment of postural imbalance. J Bone Joint Surg, [Am], 61:1182-1194, 1979

86. Mital MA: Biomechanical characteristics of the human hip joint. MS thesis, University of Strathclyde, Glasgow, 1970

87. Morris JM: Biomechanical aspect of the hip joint. Orthop Clin North Am, 2(1):33-54, 1971

88. Morsher EW: Intertrochanteric osteotomy in osteoarthrosis of the hip. In: The hip: Proc Open Scien Meet Hip Soc, pp. 24-26, 1980

89. Moseley CF: The biomechanics of the pediatric hip. Ortho Clin North Am, 11(1):3-16, 1980

90. Moser M, Hein W: Der knochen als druckstab in einem seilspanwerk, dargetelltam beispiel der hufte und der schulter. Abstr 14-15, Symposium on Wolff's law, Berlin April 1990

91. Mow VC et al: Biomechanics of diarthrodial joints: a review of twenty years of progress. J Biomech Eng., 115(4B):460-467, 1993

92. Murphy SB et al: Acetabular dysplasia in adolescent and young adult. Clin Orthop, 261:215-223, 1990

93. Nap RC et al: The influence of dietary protein content on growth in giant breed dogs. Vet Comp Orthop Trauma, 6:1-8, 1993

94. Newton CD: Osteotomy of the pelvis. In: Newton DC, Nunamaker DM eds. Textbook of small animal orthopaedics. Philadelphia, Lippincott pp. 545-548, 1985

95. Oakes MG et al: An experimental investigation of the BOP/Sertl shelf arthroplasty in the treatment of hip dysplasia (Abstract). Vet Surg, 22:394, 1993

96. Omrod AN: Treatment of hip lameness in the dog by excision of the femoral head. Vet Rec, 73:576-577, 1961

97. Olmstead ML et al: A five year study of 221 total hip replacements in the dog. J Am Vet Med Assoc, 183(2):191-194, 1983

98. Olmstead ML: Total hip replacement. Vet Clin North Am Small Anim Pract, 17:943, 1987

99. Olmstead ML: Total hip replacement in the dog. Sem Vet Med Surg, 2(2):131-140, 1987

100. Olmstead ML: The canine cemented modular total hip prosthesis. J Am Anim Hosp Assoc, 31(2),109-124, 1995

101. Ortolani M: Congenital hip dysplasia in the light of early and very early diagnosis. Clin Orthop 119:6-10, 1976

102. Page AE et al: Determination of loading parameters in the canine hip in vivo. J Biom, 26(4):571-579, 1993

103. Palmoski MJ, Brandt KD: In vivo effect of aspirin on canine osteoarthritic cartilage. Arthritis Rheum, 26(8):994-1001, 1983

104. Paul HA, Bargar WL: A modified technique for total hip replacement. J Am Anim Hosp Assoc, 23:13-18, 1987

105. Pauwels F: Der schenkelhalsbruch ein mechanisches problem. Stuttgart, F Enke Verlag, 1935

106. Pauwels F: Des affections de la hanche d'origine mechanique et de leur traitement par l'osteotomie d'adduction. Rev Chir Orthop, 37:22, 1951

107. Pauwels F: Neue richtlinien fur die operative behandlung der koxarthrose. Stuttgard, F Enke Verlag, 1961

108. Pauwels F: Gesommelte abhandlungen zur funktionellen anatomie des bewegugs apparates. New York, Springer Verlag, 1965

109. Pauwels F: Biomechanics of the normal and diseased hip. Berlin, Springer, 1976

110. Pauwels F: Biomechanics of the locomotor apparatus. Berlin, Springer, 1980

111. Pemberton PA: Pericapsular osteotomy of the ilium for treatment of congenital subluxation and dislocation of the hip. J Bone Joint Surg, [Am], 67:842-850, 1965

112. Pijanowski GJ et al: In vitro analysis of two pelvic osteotomy techniques. Vet Surg, 10(6):139-142, 1981

113. Poss R: The role of osteotomy in the treatment of osteoarthritis of the hip. J Bone and Joint Surg, [Am], 66(1):144-151, 1984

114. Prieur WD: Coxarthrosis in the dog. Part1: Normal and abnormal biomechanics of the hip joint. Vet Surg, 9(4):145-149, 1980

115. Probst CW et al: Technique for measuring the area of canine articular surfaces. Am J Vet Res, 48(4):608-609, 1987

116. Prostredny JM, Toombs JP, VanSickle DC: Effect of two muscle sling techniques on early morbidity after femoral head and neck excision in dogs. Vet Surg, 20(5):298-305, 1991

117. Rab GT: Biomechanical aspects of Salter osteotomy. Clin Orthop, 132:82-87, 1978

118. Radin EL, Paul IL: The biomechanics of the congenital dislocated hips and their treatment. Clin Orthop, 89:32-38, 1974

119. Radin EL: Biomechanics of the human hip. Clin Orthop, 152:28-34, 1980

120. Remedios AM, Fries CL: Implant complications in 20 triple pelvic osteotomies. Vet Comp Orthop Trauma, 6:202-207, 1993

121. Remedios AM, Fries CL: Treatment of canine hip dysplasia: a review. Can Vet J, 36:503-509, 1995

122. Rettenmaier JL, Constantinescu GM: Canine hip dysplasia. Compendium, 13(4):643-654, 1991

123. Richardson DC: The role of nutrition in canine hip dysplasia. Vet Clin North Am Small Anim Pract, 22(3):529-540, 1992

124. Riser WH, Shirer JF: Hip dysplasia: coxofemoral abnormalities in neonatal German shepherd dogs. J Small Anim Pract, 7:7-12, 1966

125. Riser WH, Shirer JF: Correlation between canine hip dysplasia and muscle mass: a study of 95 dogs. Am J Vet Res, 28:769-777, 1967

126. Riser WH: Canine hip dysplasia: cause and control. J AM Vet Med Assoc, 165(4):360-362, 1974

127. Riser WH: Surgically induced hip dysplasia. Vet Pathol, 12:306-315, 1975

128. Riser WH: The dog as a model for the study of hip dysplasia: some aspects of growth, form and development of the normal and dysplastic hip joint. J Vet Pathol, 12:234-334, 1975

129. Riser WH et al: Hip dysplasia. In: Newton CD, Nunamaker DM, eds. Textbook of Small Animal Orthopaedics. Philadelphia, JB Lippincott, pp. 953-980, 1985

130. Riser WH: A half century of canine hip dysplasia. Sem Vet Med Surg, 2(2):87-91, 1987

131. Riser WH: Canine hip dysplasia. In: MJ Bojrab, ed. Disease mechanism in small animal surgery, 2nd ed. Philadelphia, Lea & Febiger, pp. 797-803, 1993

132. Ronsky JL et al: In vivo quantification of the cat femoropatellar joint contact stresses and areas. J Biomech, 28(8):977-983, 1995

133. Rumph PF, Hathcock JT: A symmetric axis-based method for measuring the projected femoral angle of inclination in dogs. Vet Surg, 19(5):328-333, 1990

134. Rydell N: Biomechanics of the hip joint. Clin Orthop, 92:6-15, 1973

135. Rydell N: Forces acting on the femoral head prosthesis. Acta Orthop Scand, Suppl 88, 1966

136. Salter RB: Innominate osteotomy in the treatment of congenital dislocation and subluxation of the hip. J Bone Jt Surg, [Br], 43:518-539, 1961

137. Salter RB: Role of innominate osteotomy in the treatment of congenital dislocation and subluxation of the hip in older child. J Bone Joint Surg, [Am], 48:1413-1439, 1966

138. Salter RB, Dubos JP: The first fifteen years' personal experience with innominate osteotomy in the treatment of congenital dislocation and subluxation of the hip. Clin Orthop 98:72-103, 1974

139. Schrader SC: Triple osteotomy of the pelvis as a treatment for canine hip dysplasia. J Am Vet Med Assoc, 178:39-44, 1981

140. Schrader SC: Triple osteotomy of the pelvis and trochanteric osteotomy as a treatment for hip dysplasia in the immature dog: the surgical technique and results of 77 consecutive operations. J Am Vet Med Assoc, 189(6):659-665, 1986

141. Serafinov L: Biomechanical influence of the innominate osteotomy on the growth of the upper part of the femur. Clin Orthop, 98:39-40, 1974

142. Sertl GO, Jensen DJ: Biocompatible osteoconductive polymer (BOP) shelf arthroplasty for the surgical treatment of hip dysplasia. In: Whittick WG, ed. Canine Orthopaedics, 2nd ed. Philadelphia, Lea & Febiger, pp481-490, 1990

143. Shepherd J: Canine hip dysplasia, aetiology, pathogenesis and eradication. Aust Vet Pract, 16:71-78, 1986

144. Sherrer PK et al: Determining the in vivo areas of contact in the canine shoulder. J Biomech Eng., 101:271-278, 1979

145. Simon WH et al: Joint congruence: a correlation of joint congruence and thickness of articular cartilage in dogs. J Bone Joint Surg, [Am], 55(8):1614-20, 1973

146. Singerman RJ et al: Quantification of pressure-sensitive films using digital image scanning. Exp Mech, 27:99-103, 1987

147. Slocum B, Devine T: Pelvic osteotomy technique for axial rotation of the acetabular segment in the dogs. J Am Anim Hosp Assoc, 22:331-338, 1986

148. Slocum B, Devine T: Pelvic osteotomy in the dog as a treatment for hip dysplasia. Sem Vet Med Surg, 2(2):107-116, 1987

149. Slocum B, Devine T: Dorsal acetabular rim radiographic view for evaluation of the canine hip. J Am Anim Hosp Assoc, 26:289-296, 1990

150. Slocum B, Devine T: Pelvic osteotomy for axial rotation of the acetabular segment in dogs with hip dysplasia. Vet Clin North Am Small Anim Pract, 22(3):645-682, 1992

151. Smith C: Treatments for hip dysplasia spark controversy. J Am Vet Med Assoc, 201:205-209, 1992

152. Smith GK et al: New concepts of coxofemoral joint stability and the development of a clinical stress-radiographic method for quantitating hip joint laxity in the dog. J Am Vet Med Assoc, 196(1):59-70, 1990

153. Smith GK et al: Coxofemoral joint laxity from distraction radiography and its contemporaneous and prospective correlation with laxity, subjective score and evidence of degenerative joint disease from conventional hip-extended radiography in dogs. Am J Vet Res, 54(7):1021-1041, 1993

154. Soslowsky LJ et al: Quantification of in situ contact areas at the glenohumeral joint: a biomechanical study. J Orthop Res, 10:524-534, 1992

155. Spreull JS: Excision arthroplasty as a method of treatment of hip joint diseases in the dog. Vet Rec, 73:573-576, 1961

156. Staheli LT: Acetabular dysplasia: Treatment by pelvic osteotomy. In: Marvin Steinberg, ed. The hip and its disorders. Philadelphia, WB Saunders, pp. 335-353, 1991

157. Steel HH: Triple osteotomy of the innominate bone. J Bone Joint Surg, [Am], 55:343-350, 1973

158. Steinberg A: Kinesiology of the human body. Charles C Thomas publisher, Springfield, Illinois, 1955

159. Stoll S et al: Pelvic osteotomy for the correction of hip dysplasia. Proc Annu Meet Vet Orthop Soc, 1978

160. Stormont TJ et al: Elbow joint contact study: comparison of techniques. J Biomech, 18(5):329-336, 1985

161. Sukhiani HR et al: Pelvic canal narrowing caused by triple pelvic osteotomy in the dog. Part 1: The effect of pubic remnant length and angle of acetabular rotation. Vet Comp Orthop Trauma, 7:110-113, 1994

162. Sukhiani HR et al: Pelvic canal narrowing caused by triple pelvic osteotomy in the dog. Part 2: A comparison of three pubic osteotomy techniques. Vet Comp Orthop Trauma, 7:114-117, 1994

163. Sutherland DH, Greenfield R: Double innominate osteotomy. J Bone Joint Surg, [Am], 59:1082-1091, 1977

164. Tarvin G, Lippincott CL: Excision arthroplasty for the treatment of canine hip dysplasia using the biceps femoris muscle. Sem Vet Med Surg, 2(2):158-160, 1987

165. Tomlison J, McLaughlin R: Medically managing canine hip dysplasia. Vet Med, 1:48-53, 1996

166. Tonnis D et al: A modified technique of the triple pelvic osteotomy: early results. J Pediatr Orthop, 1:241-249, 1981

167. Trevor PB et al: Evaluation of biocompatible osteoconductive polymer as an orthopaedic implant in dogs. J Am Vet Med Assoc, 200:1651-1661, 1992

168. Vasseur PB et al: Evaluation of carpofen, a nonsteroidal anti-inflamatory drug for osteoarthritis in dogs (Abst.). Vet Surg, 21:409, 1992

169. Wagner H: Experiences with spherical acetabular osteotomy for the correction of the dysplastic hip. In: Weil UH, ed. Progress in Orthopaedic Surgery, 2nd ed. New York, Springer Verlag, 1978

170. Walker TL, Prieur WD: Intertrochanteric femoral osteotomy. Sem Vet Med Surg, 2(2):117-130, 1987

171. Wallace LJ: Pectineus tendonectomy or tenotomy for treating clinical canine hip dysplasia. Vet Clin North Am Small Anim Pract, 1:455-465, 1971

172. Wallace LJ: Canine hip dysplasia, past and present. Sem Vet Med Surg, 2(2):92-106, 1987

173. Wiberg G: Studies on dysplastic acetabula and congenital subluxation of the hip joint with special reference to the complications of osteoarthritis. Acta Chir Scand 83(suppl):58, 1939

174. Wiberg G: Roentgenographic and anatomic studies on the femoropatellar joint. Acta Orthop Scand, 12:319-410, 1941

175. Wilfrid E et al: Properties of body segments based on size and weight. Am J Anat, 120(1):33-54, 1967

176. White KK et al: Contact studies of the femoropatellar joint. Am J Vet Res, 43(3):429-435, 1982

177. Yao JQ, Seedhom BB: A new technique for measuring areas in human joints - The “3S technique”. Proc Instn Mech Engrs, 205:69-72, 1991

178. Zolton GM: A review of 23 bilateral triple pelvic osteotomies. Proc Annu Meet Vet Orthop Soc, p 15, 1991